Building High-Quality Climate Data Records from Operational Satellites

Fuzhong Weng

NOAA Center for Satellite Applications and Research

Outline

- Background on Climate Trend Analysis

- Instrument CalVal for Advanced Weather and Climate Reserach

- New Analysis of Atmospheric Temperature Trend from MSU and AMSU through non-Linear Trending

- Effects of Clouds and Precipitation on AMSU Derived Climate Trending

- Atmospheric Temperature Trend from 1DVar Retrieval

- Summary and Conclusions

Background on Climate Trend Analysis

Detection of Climate Trend and Its Sensitivity to Measurement Precision

Given an observed time series: $\left\{ x_i^o, i = 1, 2, \ldots, N \right\}$

Using a linear-regression model: $x^m = a(t - \bar{t})$

True value of variable x at any time: $x^t = x^m + \varepsilon_m \equiv a(t - \bar{t}) + \varepsilon_m$

The observed time series: $x^o = x^t + \varepsilon_o \equiv a(t - \bar{t}) + \varepsilon_m + \varepsilon_o$

which can be expressed in a matrix form : $\mathbf{x}^o = \mathbf{A}a + \boldsymbol{\varepsilon}$

where:

$$\mathbf{x}^o = \begin{pmatrix} x_1^o \\ x_2^o \\ \ldots \\ x_N^o \end{pmatrix} \qquad \mathbf{A} = \begin{pmatrix} t_1 - \bar{t} \\ t_2 - \bar{t} \\ \ldots \\ t_N - \bar{t} \end{pmatrix} \qquad \boldsymbol{\varepsilon} = \begin{pmatrix} \varepsilon_{m,1} + \varepsilon_{o,1} \\ \varepsilon_{m,2} + \varepsilon_{o,2} \\ \ldots \\ \varepsilon_{n,N} + \varepsilon_{o,N} \end{pmatrix}$$

Detection of Climate Trend and Its Sensitivity to Measurement Precision

The linear regression coefficient (*a*) is obtained by a least-square fit which minimizes the difference between observations and linear regression model:

$$J = (\mathbf{x}^o - \mathbf{A}a)^T (\mathbf{x}^o - \mathbf{A}a)$$

For a twelve month/year time series: we can obtain the trend as

$$a = \frac{12 \sum_{i=1}^{N} x_i^o \left(t_i - \overline{t} \right)}{\left(N^3 - N \right)}$$
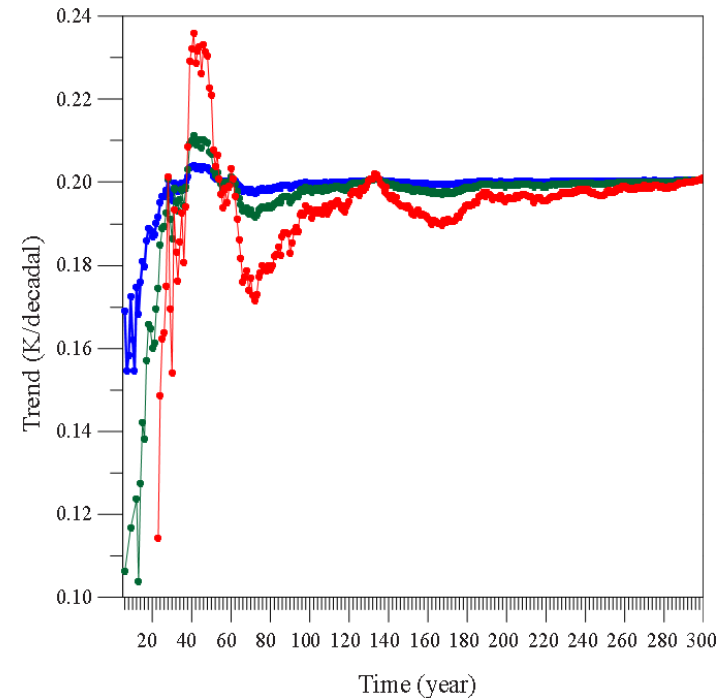
Fig. 1 Climate trend calculated from different lengths of time series with three different observation error variances: 0.1K (blue line), 0.3K (green line) and 1K (red line)

Climate Trend Error from Observations

The uncertainty of the trend is

$$\sigma_a^2 = \frac{12\left(\sigma_o^2 + \sigma_n^2\right)}{N^3 - N}$$

where:

N ——————— Data length

σ_o^2 ——————— Observation error

σ_n^2 ——————— Natural variability
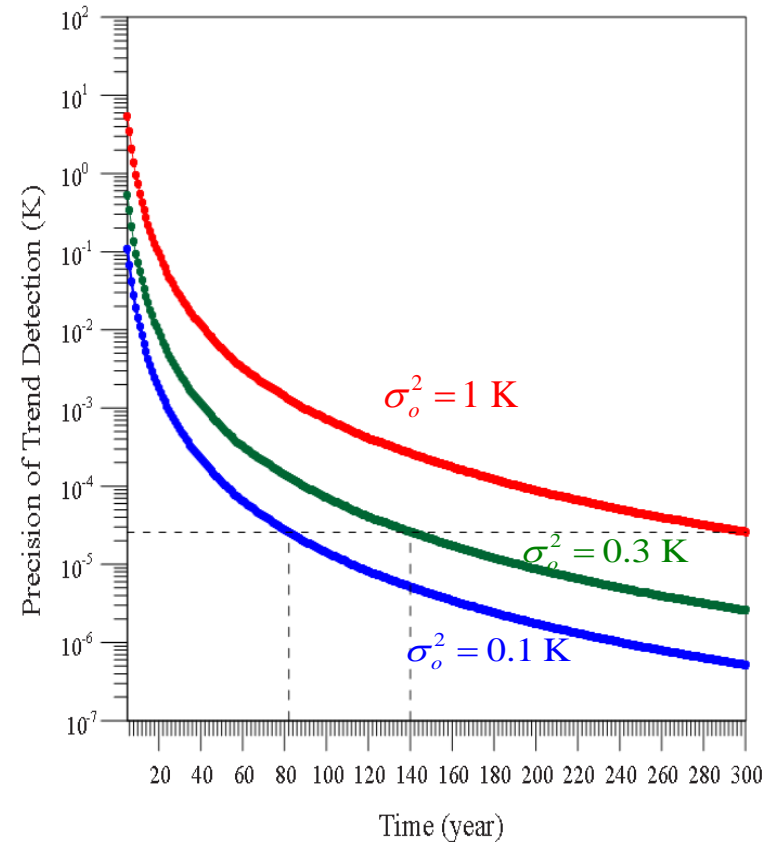
Fig. 2 Variations of σ_{trend} with respect to data length for the trends shown in Fig. 1

$\sigma_o^2 = 1$ K

$\sigma_o^2 = 0.3$ K

$\sigma_o^2 = 0.1$ K

6

Implications to Construction of Satellite Climate Data Record

- Well characterize the errors of satellite measurements through comprehensive calibration campaign

- Increase the data record length through cross-calibrating all the operational satellite data into a reference satellite through spectral, spatial and physical harmonization

- Understand the climate trend studies in thematic spaces from a comprehensive remote sensing algorithm, and compare directly with the trend study in radiance space

- Understand the natural variability using linear and non-linear trending of satellite data according to different analysis scenarios

Instrument CalVal for Advanced Weather and Climate Research

ATMS Channel Noise Characterization
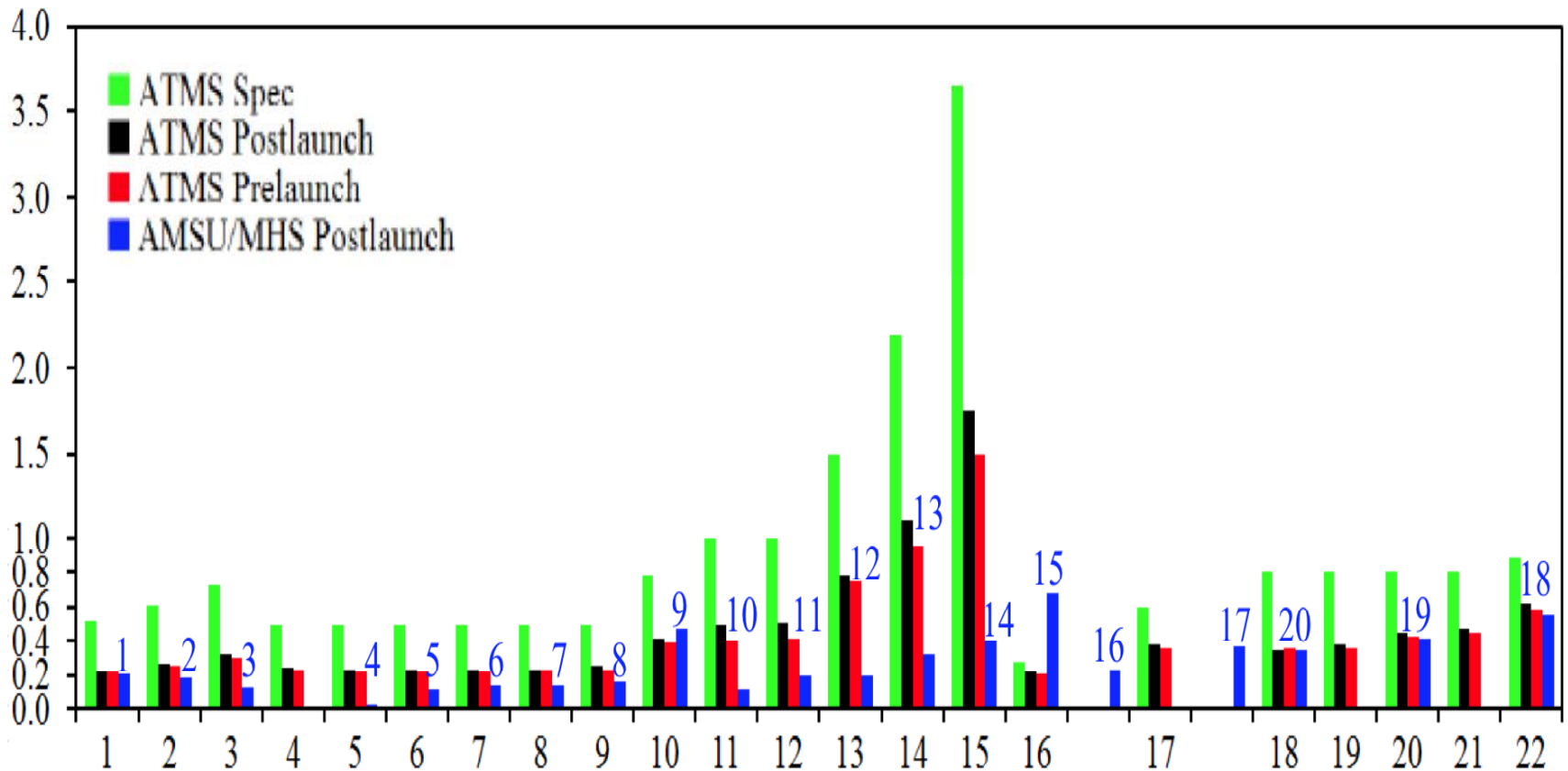
All Channels are within Specifications (Weng et al., 2012, JGR)

ATMS Pre-launch Calibration Accuracy
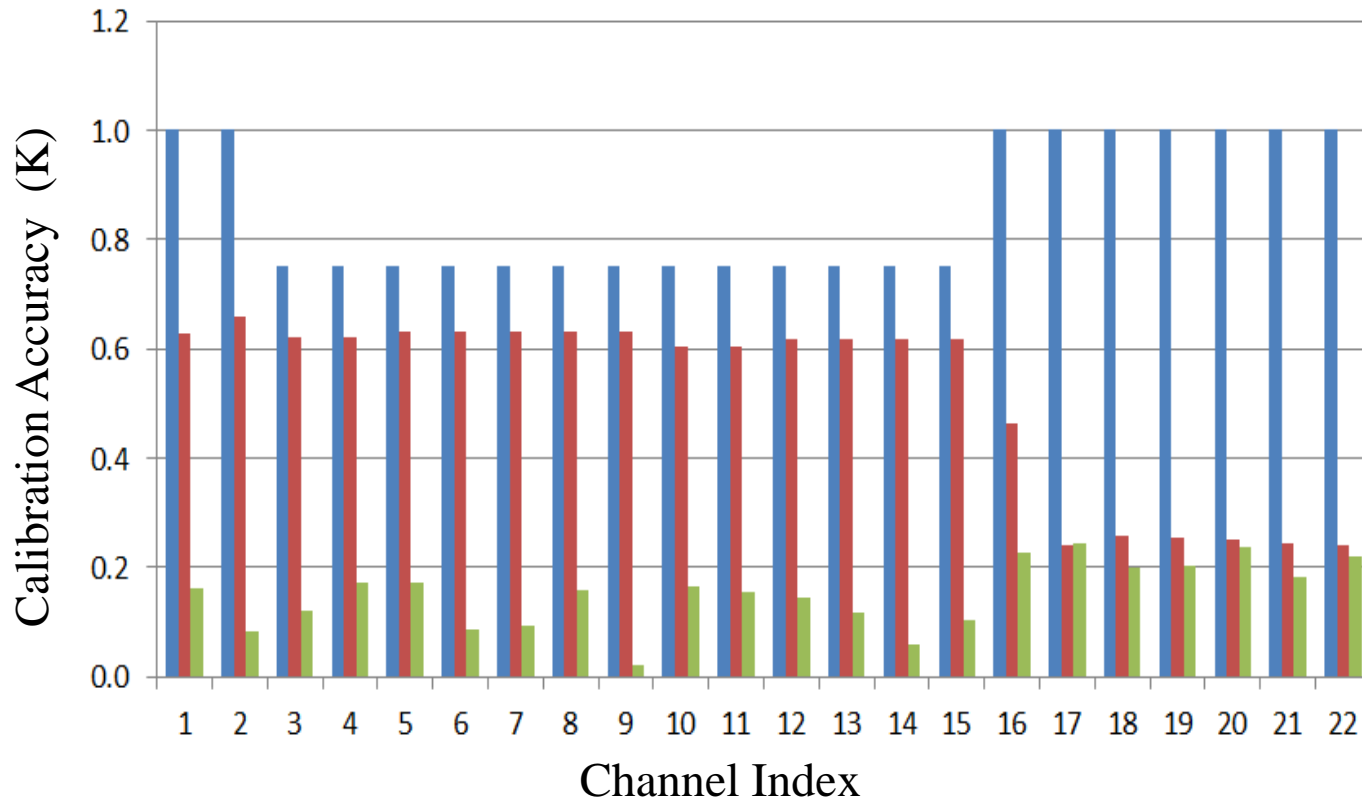
Red – Calibration accuracy from a nominal data, Green – values obtained
from prelaunch Thermal Vacuum (TVAC), and Blue – specification

ATMS Calibration Accuracy Assessment Using GPS RO

- Time period of data search:

  January, 2012

- Collocation of ATMS and COSMIC data:

  Time difference < 0.5 hour

  Spatial distance < 30 km

(GPS geolocation at 10km altitude is used for spatial collocation)

Distribution of collocated ATMS in January 2012
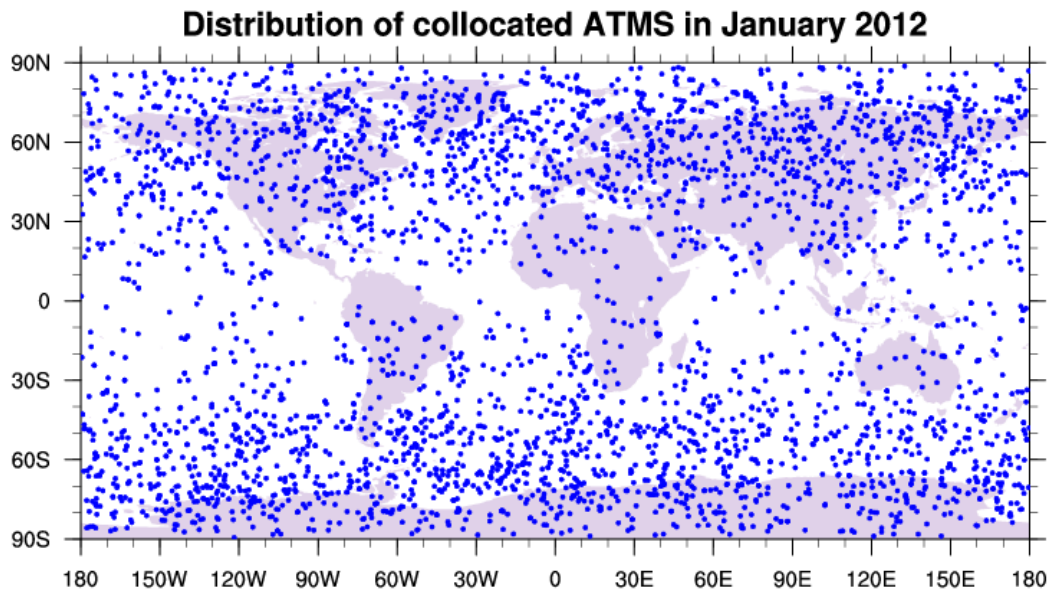
3056 collocated measurements

ATMS Bias Obs (TDR) - GPS Simulated
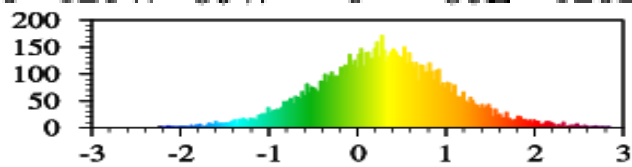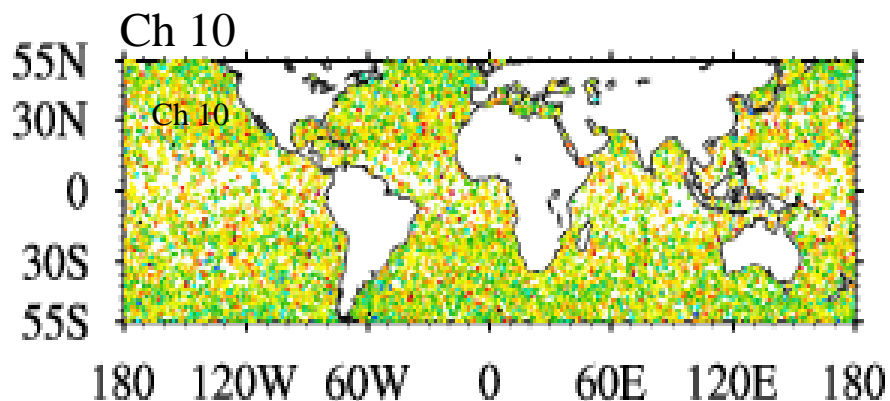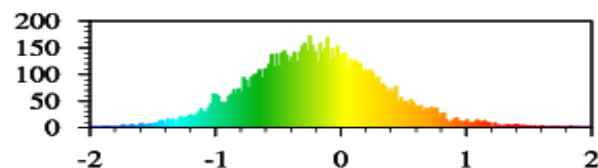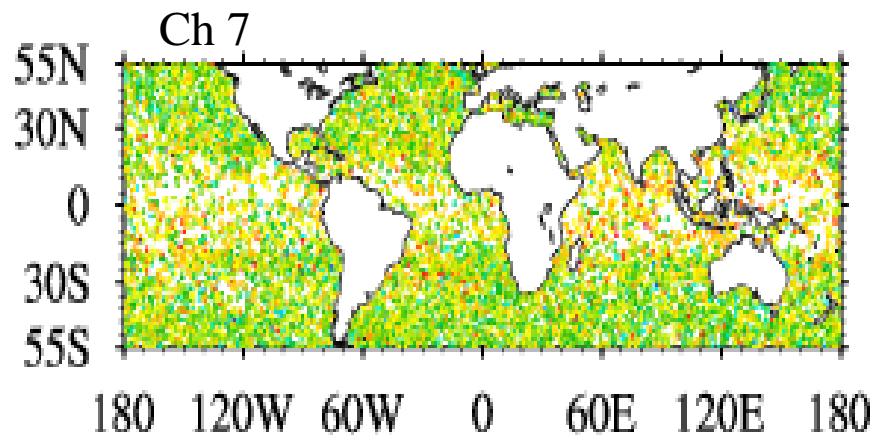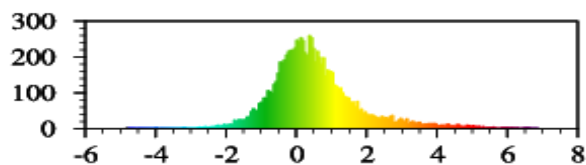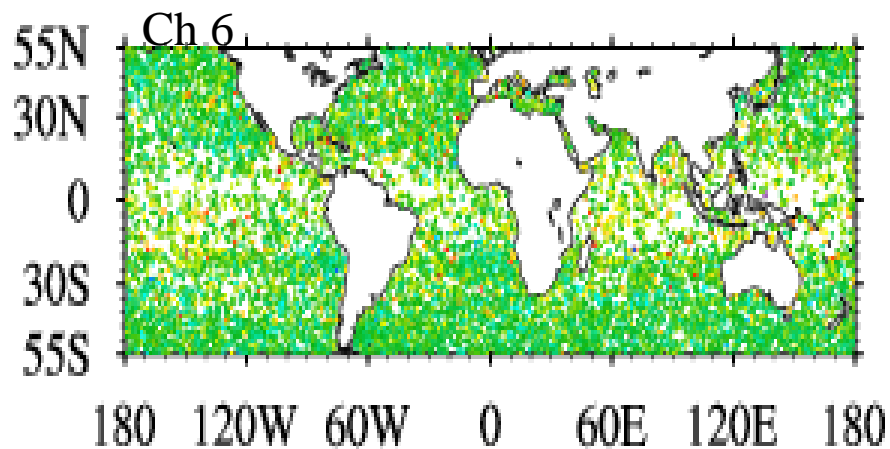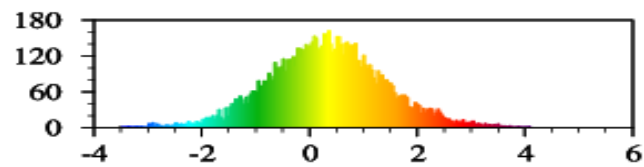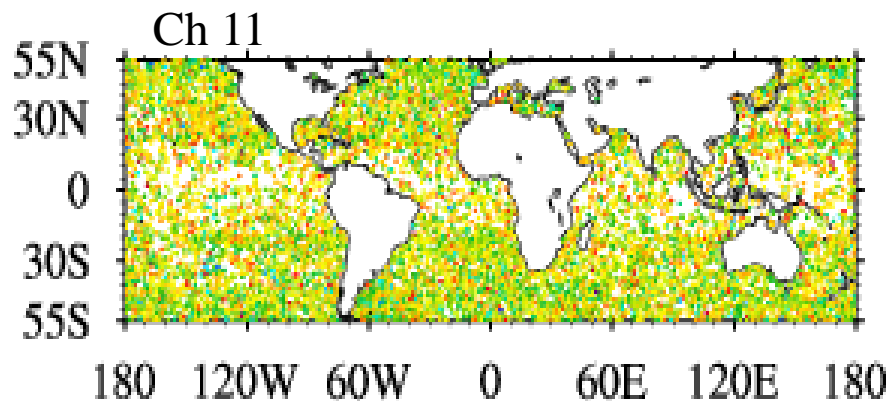
ATMS Bias Obs - Sim (GPS RO)

13
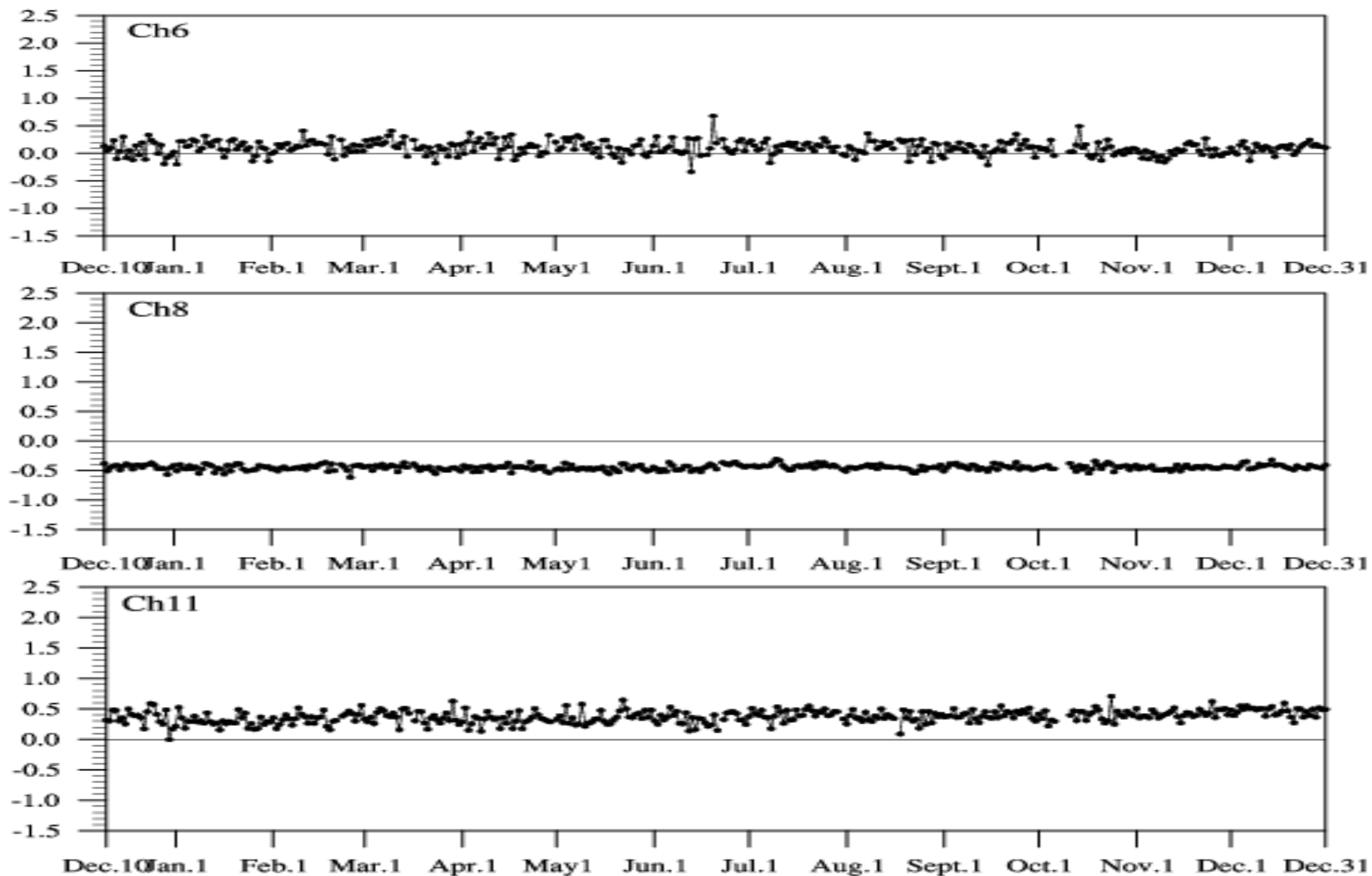
ATMS TDR-to-SDR Conversion Algorithm (1/2)

- **Methods**
  - A conversion theory was developed and tested with ATMS data
  - ATMS PCT/LUT were updated to characterize the slope and intercept
  - SDR angular dependent biases are assessed using ECMWF and CRTM simulations
  - ATMS antenna emission is investigated and a model for quantifying the emission on SDR products is being developed

- **Results**
  - ATMS SDR products have small bias for most of channels
  - ATMS SDR at WG bands are only corrected with intercept due to an uncertainty in its antenna gain efficiency

SDR (ch2)

SDR (Ch8)
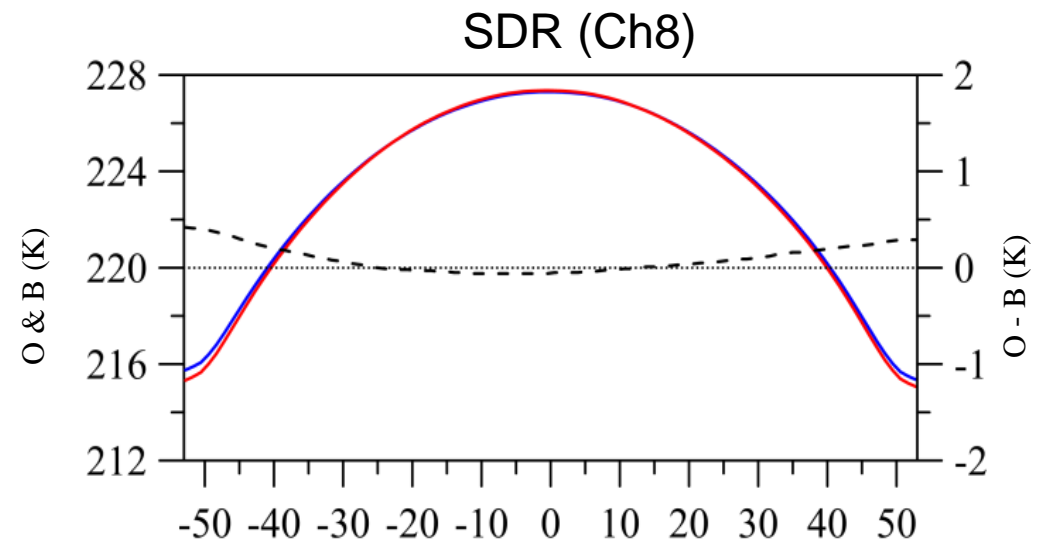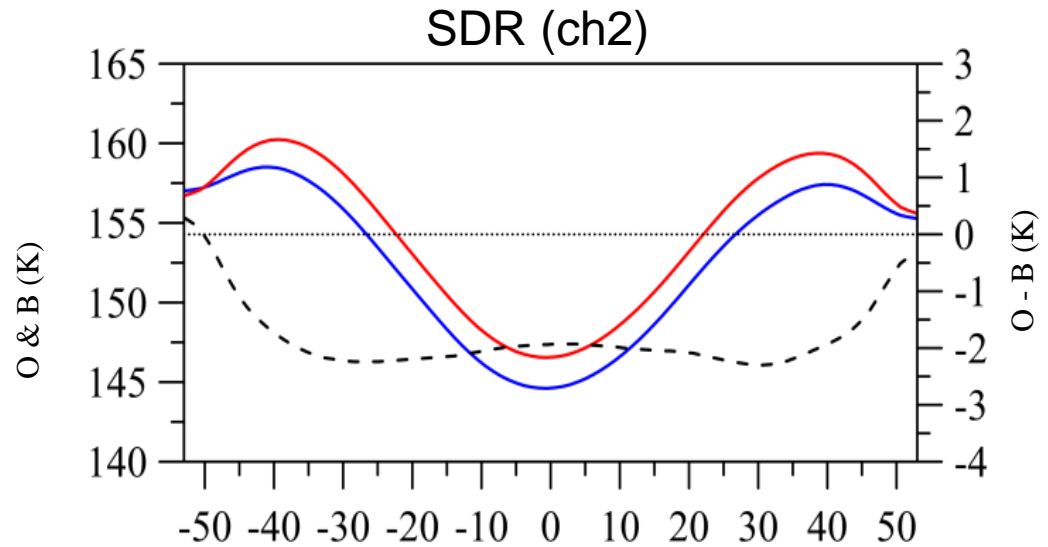
ATMS TDR-to-SDR Conversion Algorithm (2/2)
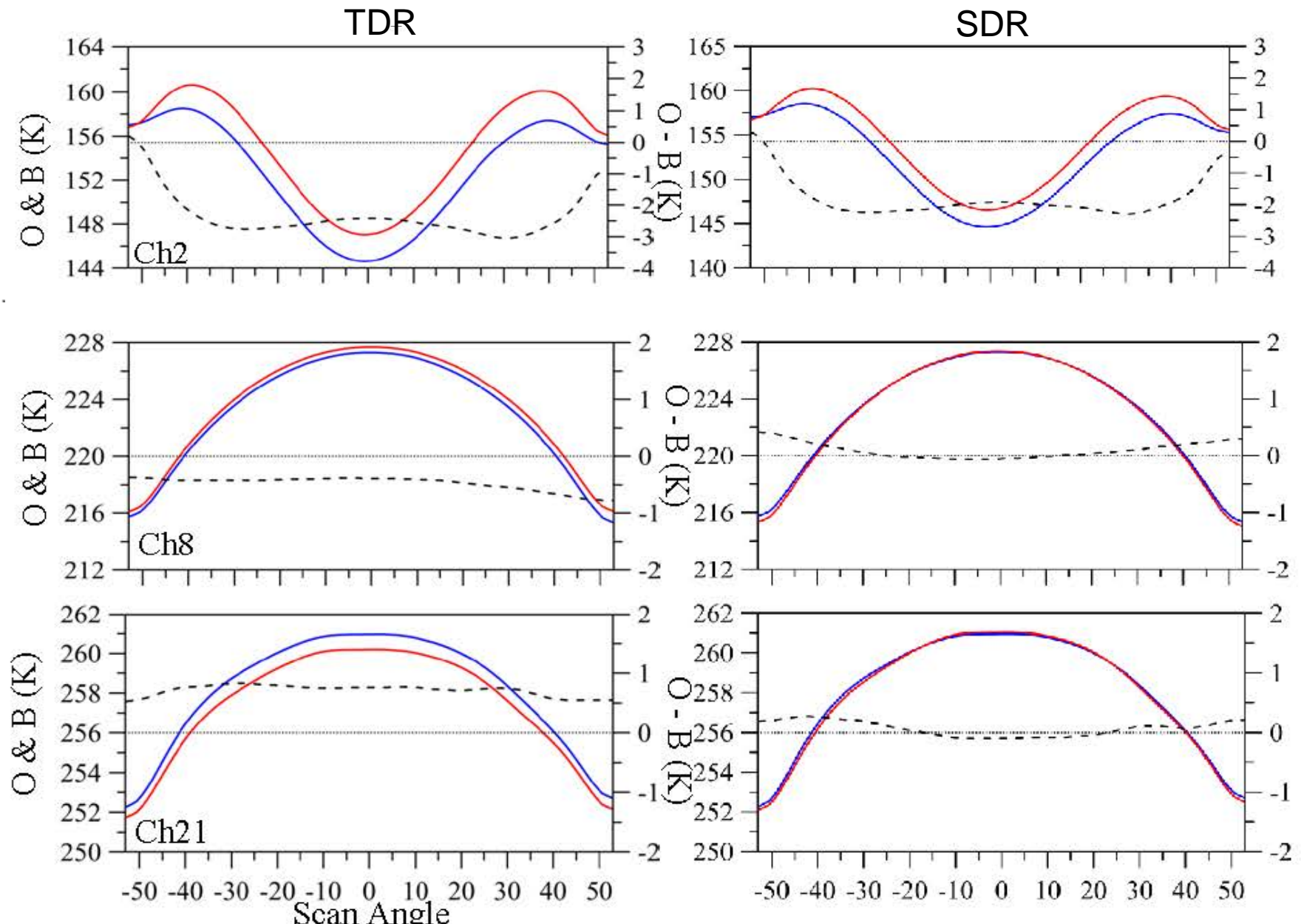
USA, China and Europe Meteorological Satellites
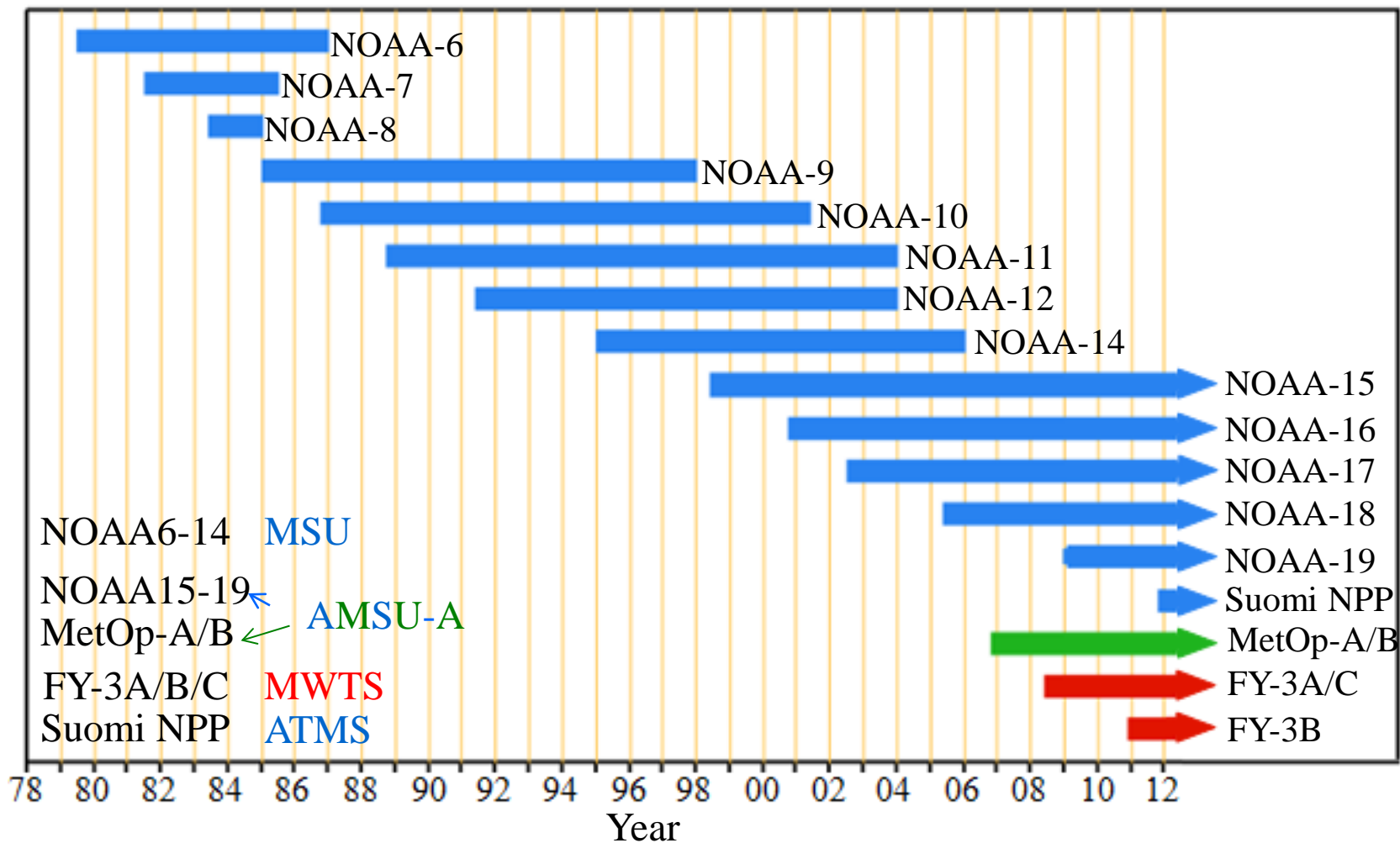
MSU			AMSU/MHS			ATMS		
Ch	**GHz**	**Pol**	**Ch**	**GHz**	**Pol**	**Ch**	**GHz**	**Pol**
			1	23.8	QV	1	23.8	QV
			2	31.399	QV	2	31.4	QV
1	50.299	QV	3	50.299	QV	3	50.3	QH
						4	51.76	QH
			4	52.8	QV	5	52.8	QH
2	53.74	QH	5	53.595 ± 0.115	QH	6	53.596 ± 0.115	QH
			6	54.4	QH	7	54.4	QH
3	54.96	QH	7	54.94	QV	8	54.94	QH
			8	55.5	QH	9	55.5	QH
4	57.95	QH	9	fo = 57.29	QH	10	fo = 57.29	QH
			10	fo $\pm$ 0.217	QH	11	fo$\pm$0.3222$\pm$0.217	QH
			11	fo$\pm$0.3222$\pm$0.048	QH	12	fo$\pm$ 0.3222$\pm$0.048	QH
			12	fo $\pm$0.3222$\pm$0.022	QH	13	fo$\pm$0.3222$\pm$0.022	QH
			13	fo$\pm$ 0.3222$\pm$0.010	QH	14	fo$\pm$0.3222 $\pm$0.010	QH
			14	fo$\pm$0.3222$\pm$0.0045	QH	15	fo$\pm$ 0.3222$\pm$0.0045	QH
			15	89.0	QV			
			16	89.0	QV	16	88.2	QV
			17	157.0	QV	17	165.5	QH
						18	183.31 ± 7	QH
						19	183.31 ± 4.5	QH
			19	183.31 ± 3	QH	20	183.31 ± 3	QH
			20	191.31	QV	21	183.31 ± 1.8	QH
			18	183.31 ± 1	QH	22	183.31 ± 1	QH

Legend:
- 🟩 Exact match to AMSU/MHS
- 🟨 Only Polarization different
- 🟧 Unique Passband
- 🟥 Unique Passband, and Pol. different from closest AMSU/MHS channels

ATMS Weighting Functions
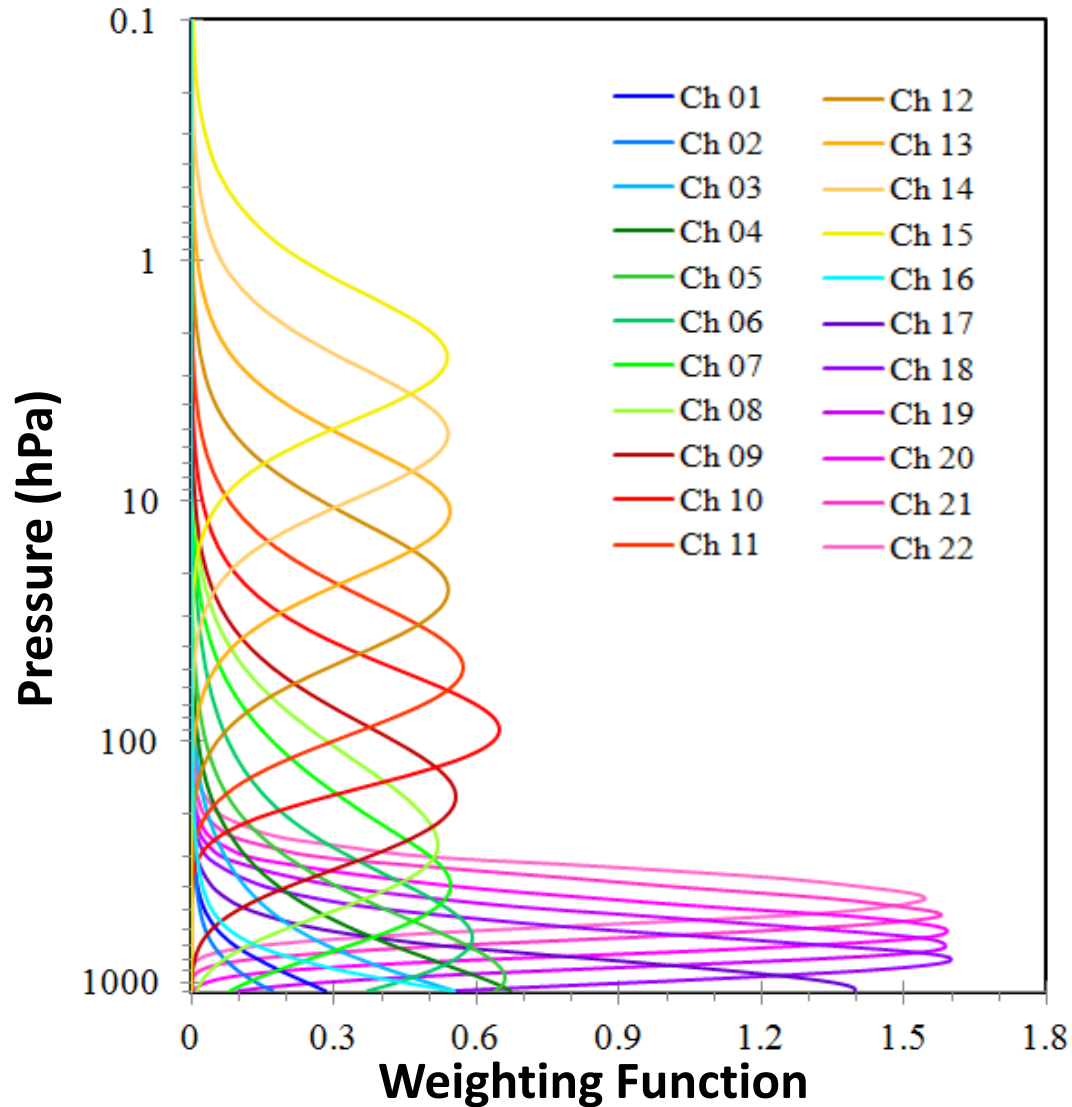
Three Generations of Microwave Sounding Instruments from MSU to AMSU/MHS to ATMS

ATMS Field of View Size for the beam width of 2.2° – black line

ATMS Resample to the Field of View Size for the beam width of 3.3°- blue line
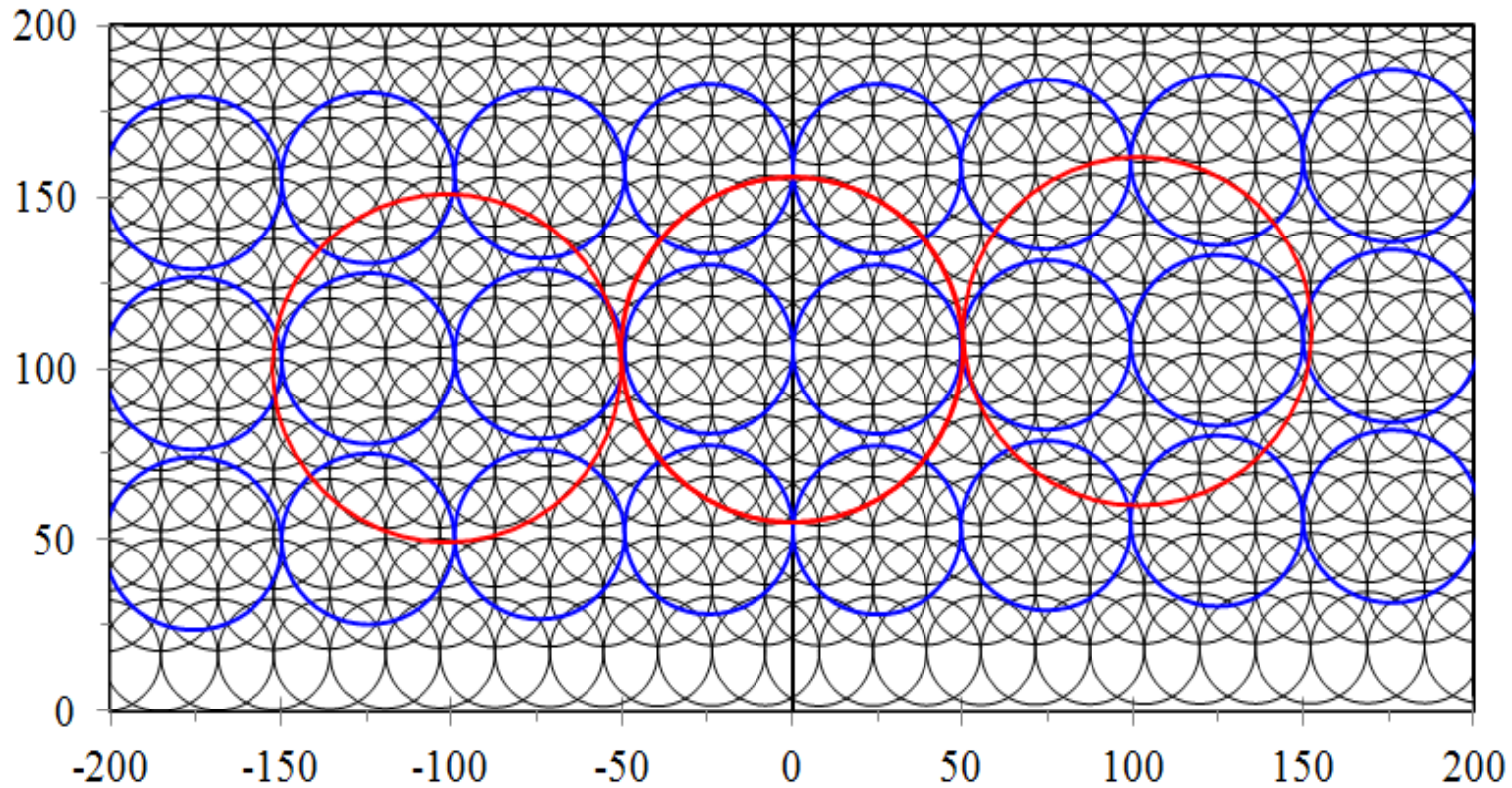
ATMS Resampling Algorithm

$$T_b^{BG}(k) = \sum_{i=-N_{ch}}^{N_{ch}} \sum_{j=-N_{ch}}^{N_{ch}} w(k+i,j) T_b^{ATMS}(k+i,j)$$

$$w(k+i,j) - \text{B-G coefficients}$$

$$N_{ch} = \begin{cases} 1 & \text{Channels 1 - 2} \\ 2 & \text{Channels 3 -16} \end{cases}$$

Stogryn, A., 1978: Estimates of brightness temperatures from scanning radiometer data. *IEEE Trans. Ant. & Prop.,* AP-26, 720-726.

Backus-Gilbert (BG) Methodology for Consistent AMSU-A and ATMS Resolution
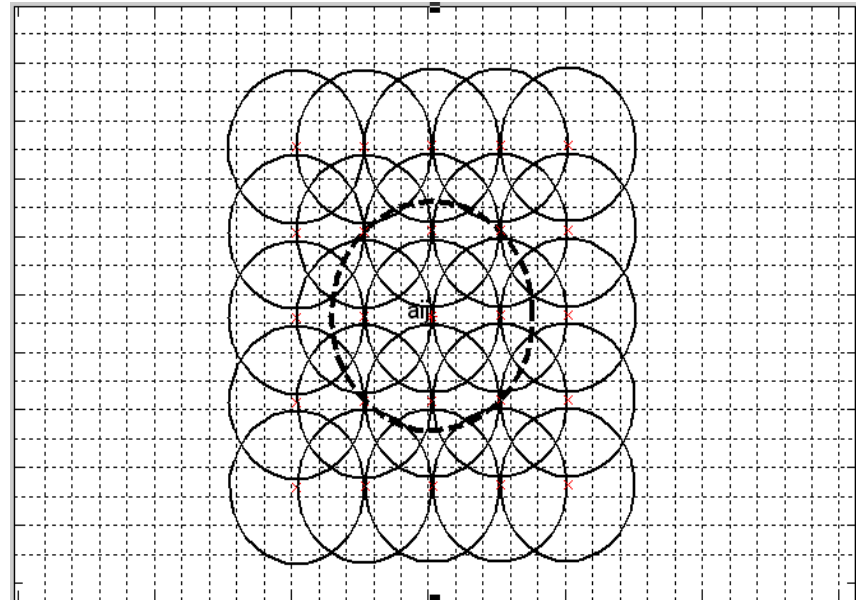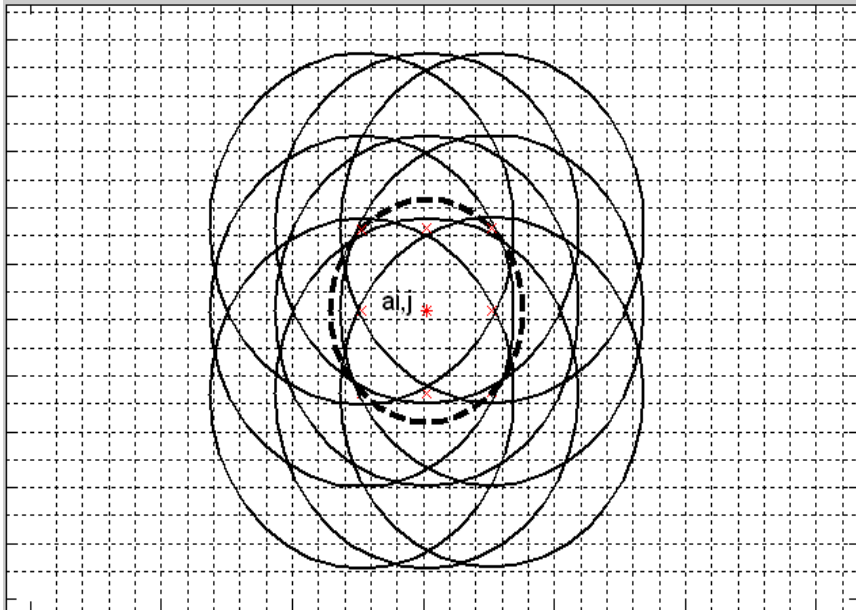
ATMS 5.2 degree beam width: 3 × 3 FOVs used for AMSU-A 3.3 degree beam width

ATMS 2.2 degree beam width: 5 × 5 FOVs used for AMSU-A 3.3 degree beam width

Backus-Gilbert (BG) Methodology for Consistent AMSU-A and ATMS Resolution near Nadir

ATMS Channels 3-16
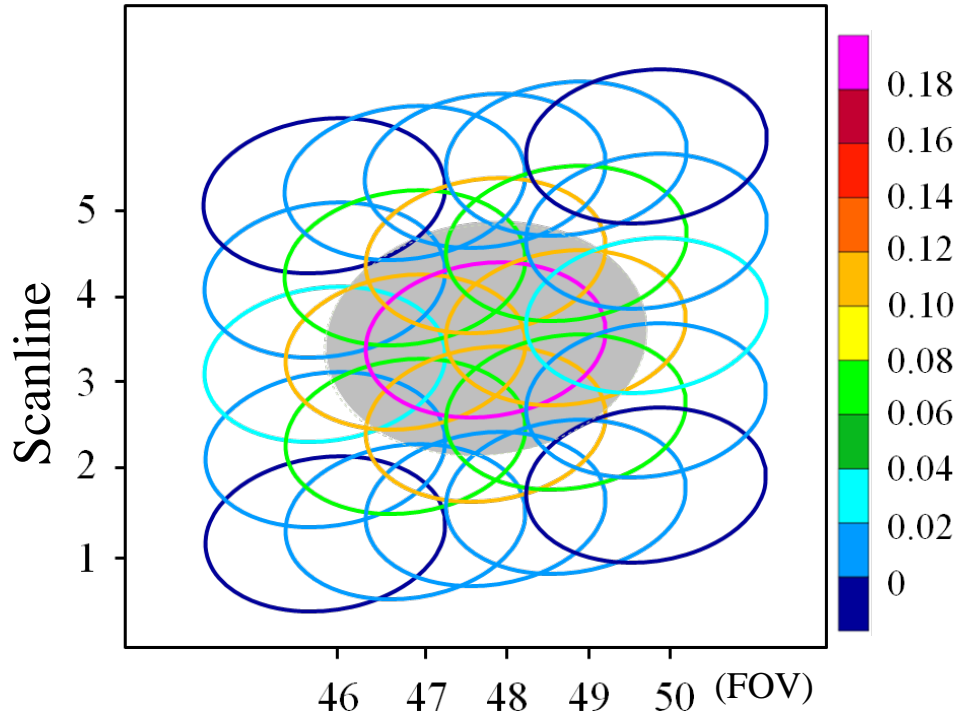
ATMS Channels 1-2
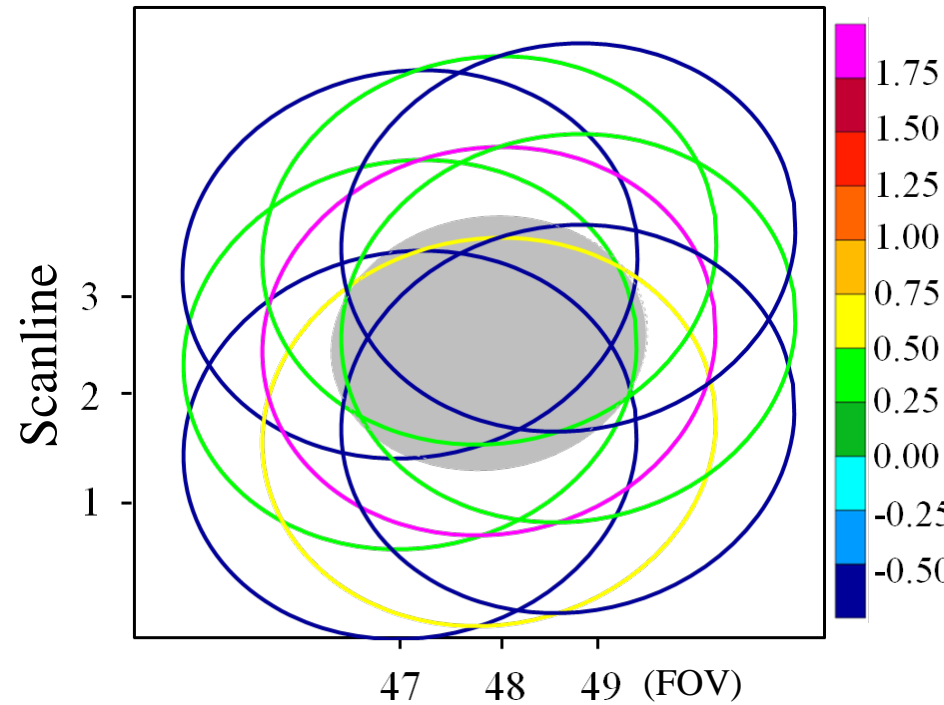
An effective AMSU-A target FOV: output of BG remap (shaded in gray)

ATMS effective FOVs: Circles with colors indicating the magnitude of BG coefficients

T_b at Channel 1 within Sandy before and after Remap
(0600 UTC October 28, 2012)

T_b
(original)
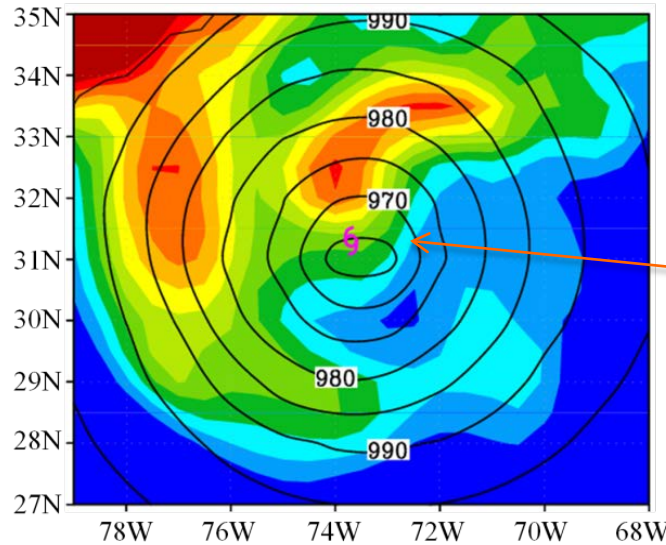
T_b^{BG}

(after BG)

NCEP GFS SLP
(contour interval: 10hPa)
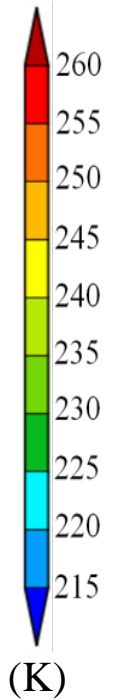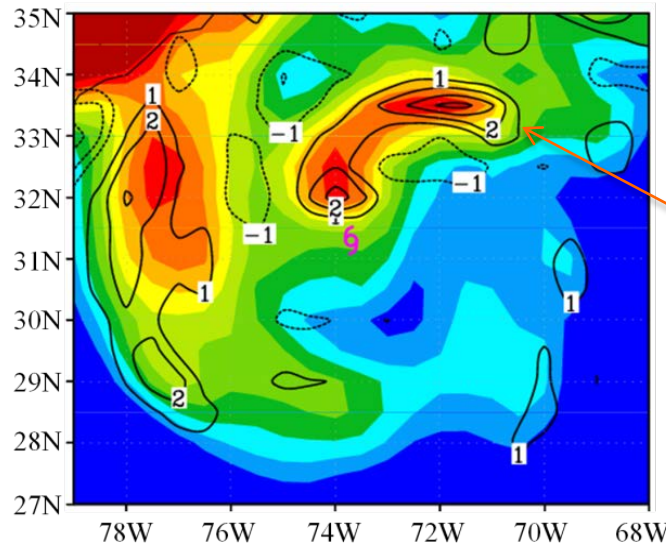
$$\Delta T_b = T_b^{BG} - T_b$$
(contour interval: 1K)

(K)

T_b at Channel 1 within Sandy before and after BG
(0600 UTC October 28, 2012)

T_b^{BG} and ΔT_b

LWP

(K)

(kg/m^2)
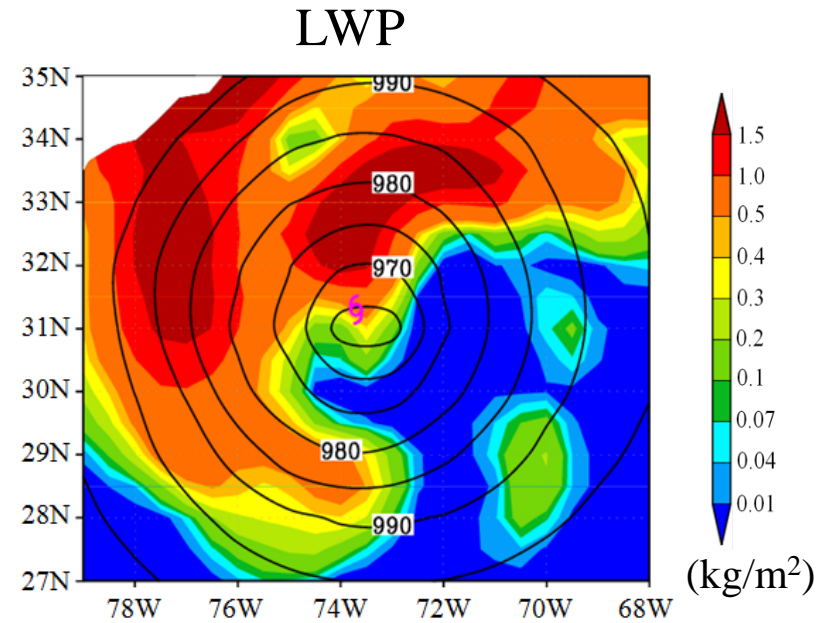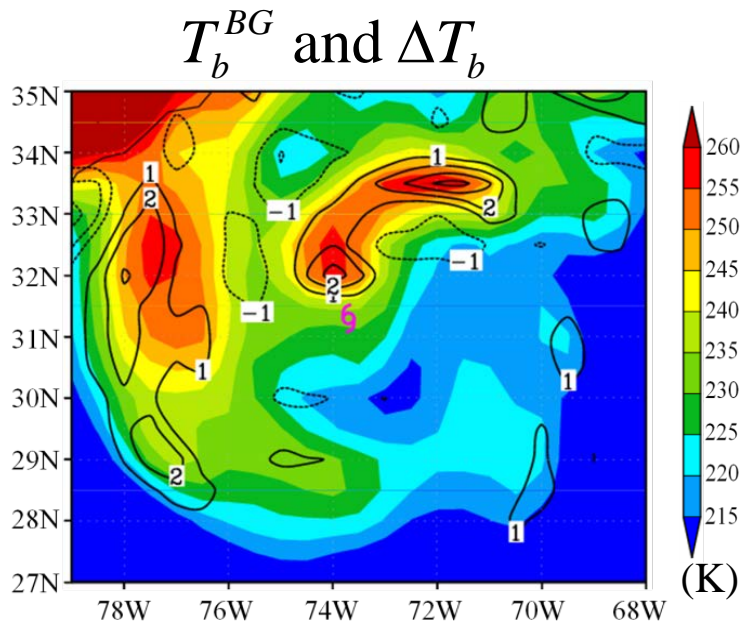
- The measured brightness temperatures at 23.8 GHz are higher over hurricane rainbands due to the contributions from cloud and water vapor emission

- The maximum brightness temperatures over cloud areas after remap are more than 2-3K lower than those before the remap

- The gradients of brightness temperatures near cloud edges become sharper

T_b at Channel 16 within Sandy before and after BG
(0600 UTC October 28, 2012)

T_b^{BG} and ΔT_b IWP
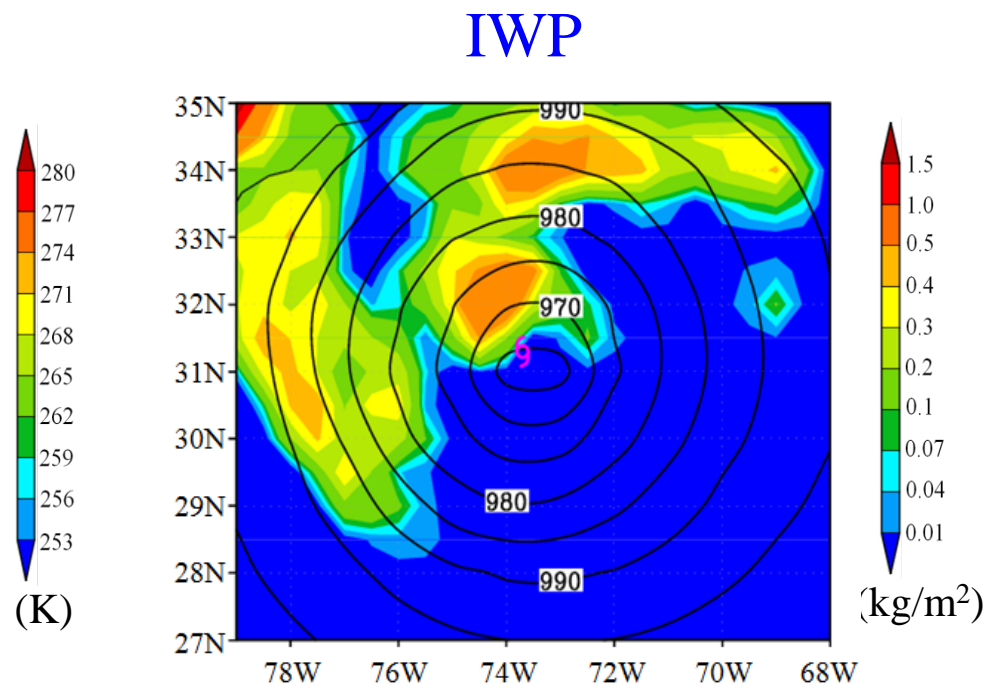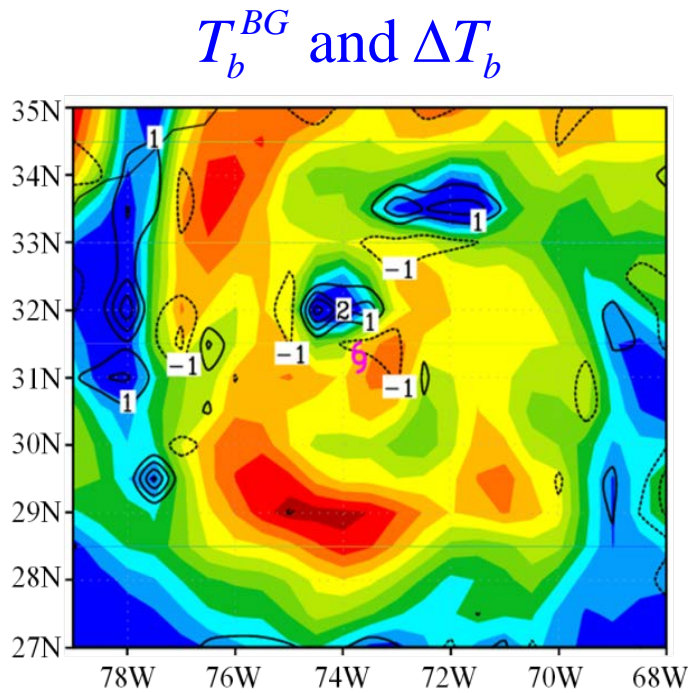
- The measured brightness temperatures at 88.2 GHz are lower over areas with ice cloud within hurricane rainbands due to ice scattering effect on radiation

- The minimum brightness temperatures over ice cloud areas after remap are more than 2-3K lower than those before the remap

Further Characterization of Bias between Resample ATMS vs. AMSU using SNO Data

Northern Hemisphere   Southern Hemisphere
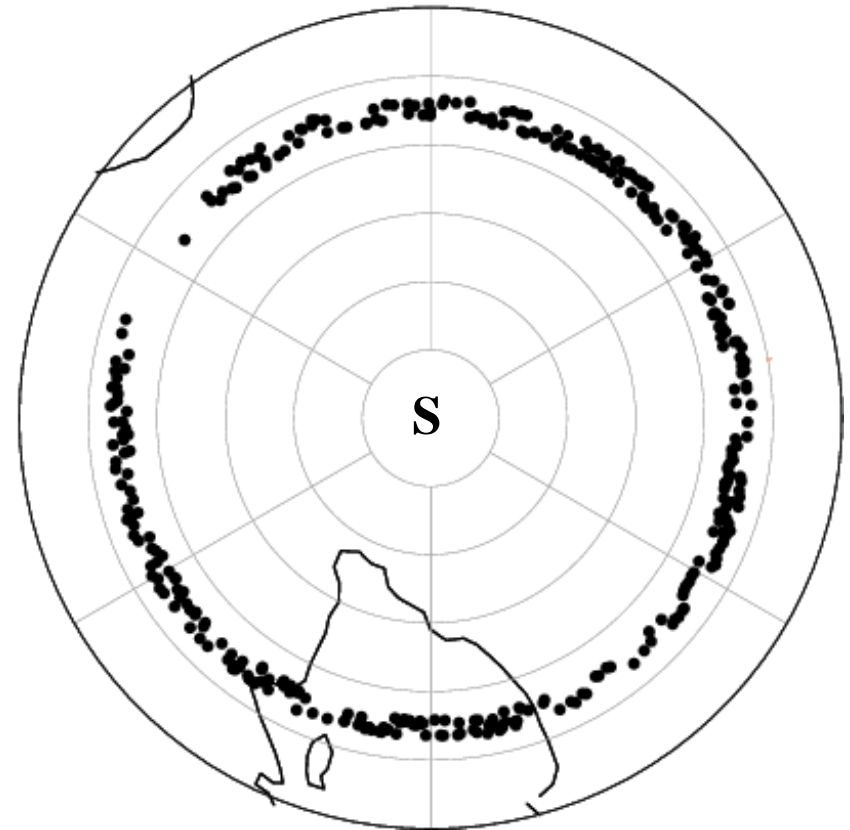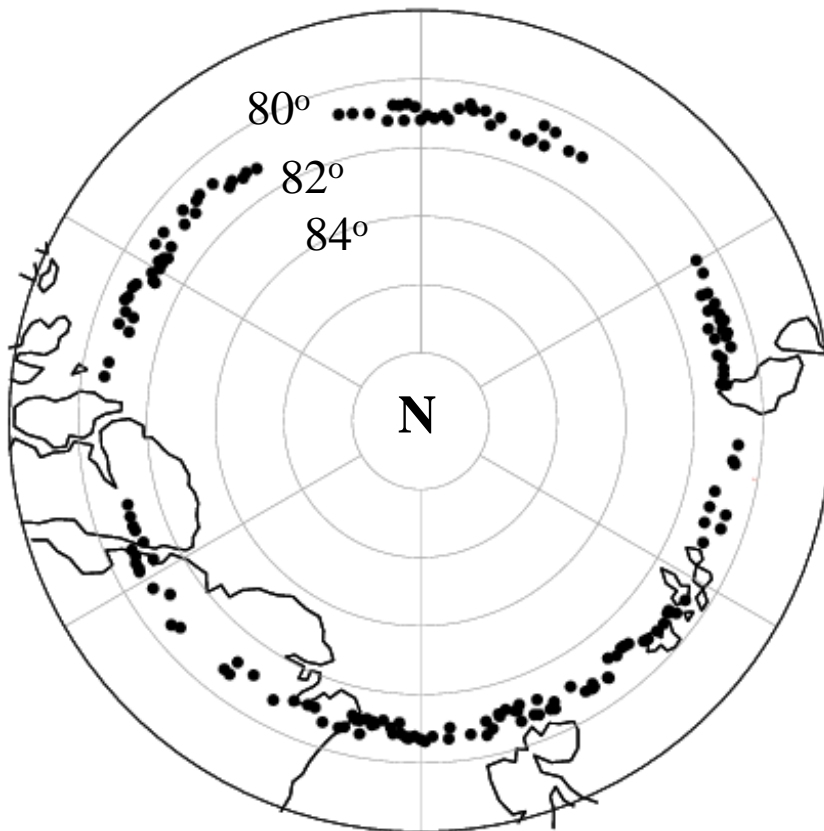
Time Period: January 1, 2012 - March 31, 2013
Collocation Criteria: 15 km and 60 seconds

Scatter Plots of $\Delta T_b (= O^{ATMS} - O^{NOAA-18})$
(Blue :Arctic and Red: Antarctic)
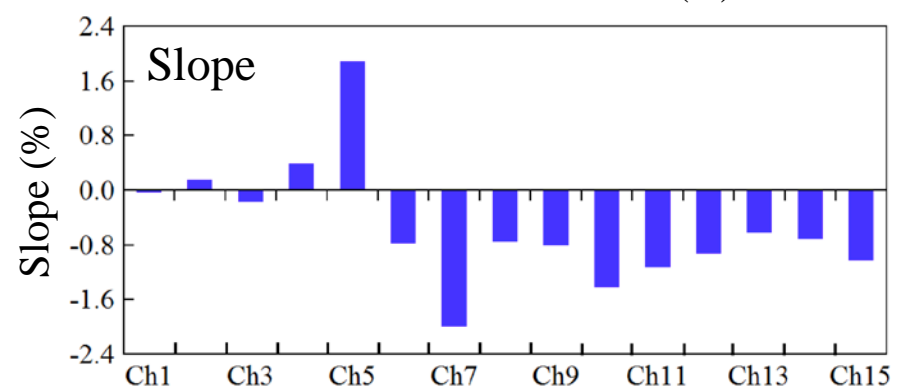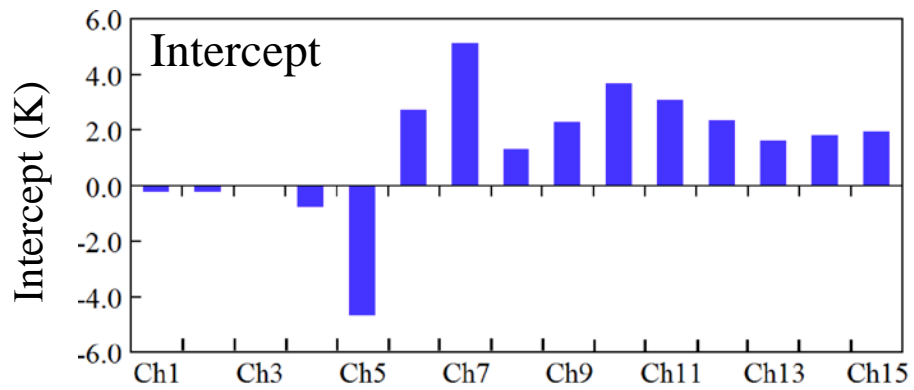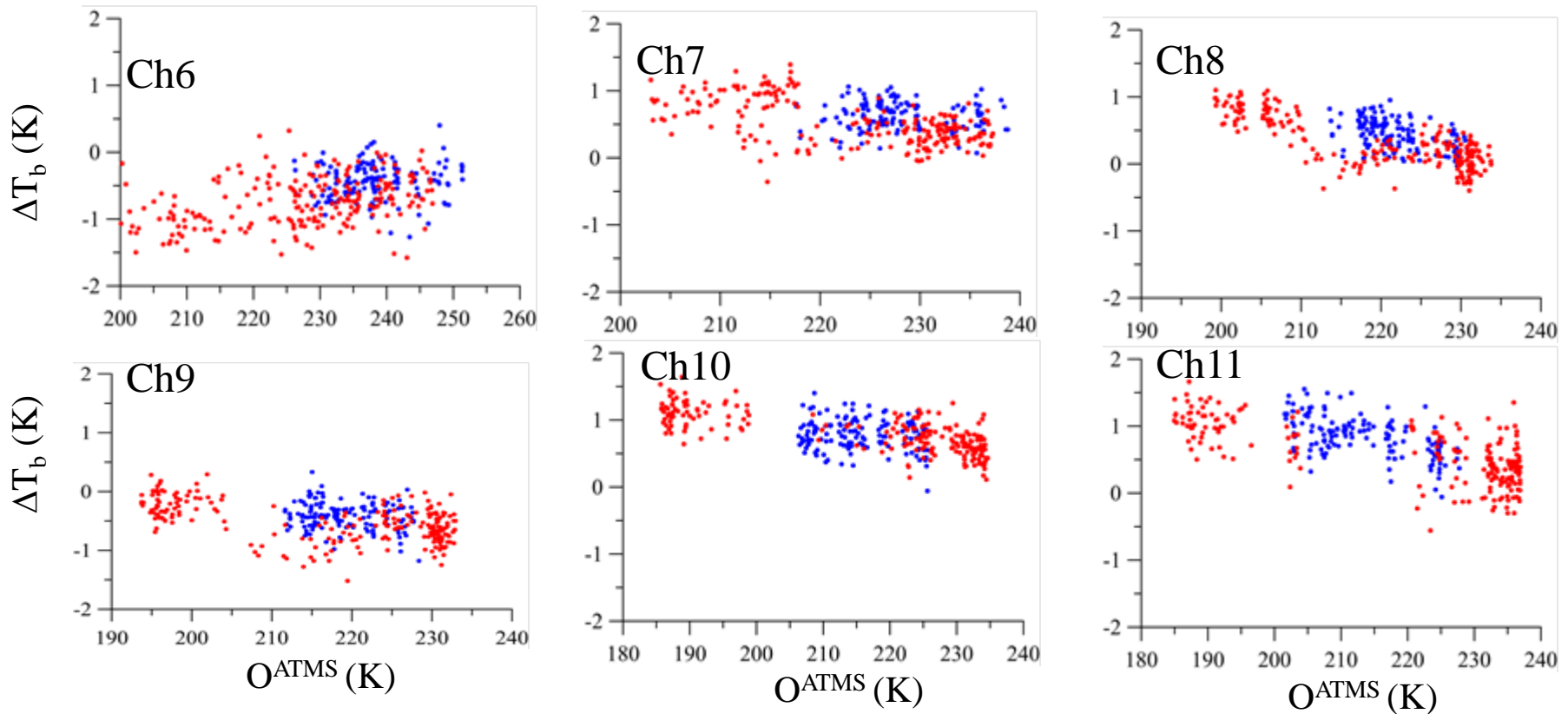
Bias between Resample ATMS and AMSU-A

Channel	ATMS remap minus NOAA-18 AMSU-A		
	mean	intercept	slope
1	-0.25	-0.22	-0.0002
2	0.08	-0.20	0.0015
3	-0.35	-0.01	-0.0016
5	0.15	-0.74	0.0039
6	-0.29	-4.66	0.0189
7	0.99	2.73	-0.0077
8	0.70	5.12	-0.0199
9	-0.30	1.31	-0.0074
10	0.58	2.29	-0.0079
11	0.59	3.66	-0.0141
12	0.60	3.06	-0.0112
13	0.26	2.35	-0.0092
14	0.18	1.61	-0.0061
15	0.08	1.82	-0.0070
16	-0.05	1.95	-0.0102

Temporal Evolution of Channel 6 Observation

NOAA-15
NOAA-18
MetOp-A
SNPP

nadir
clear-sky
(2S-2N)
(80W-100W)
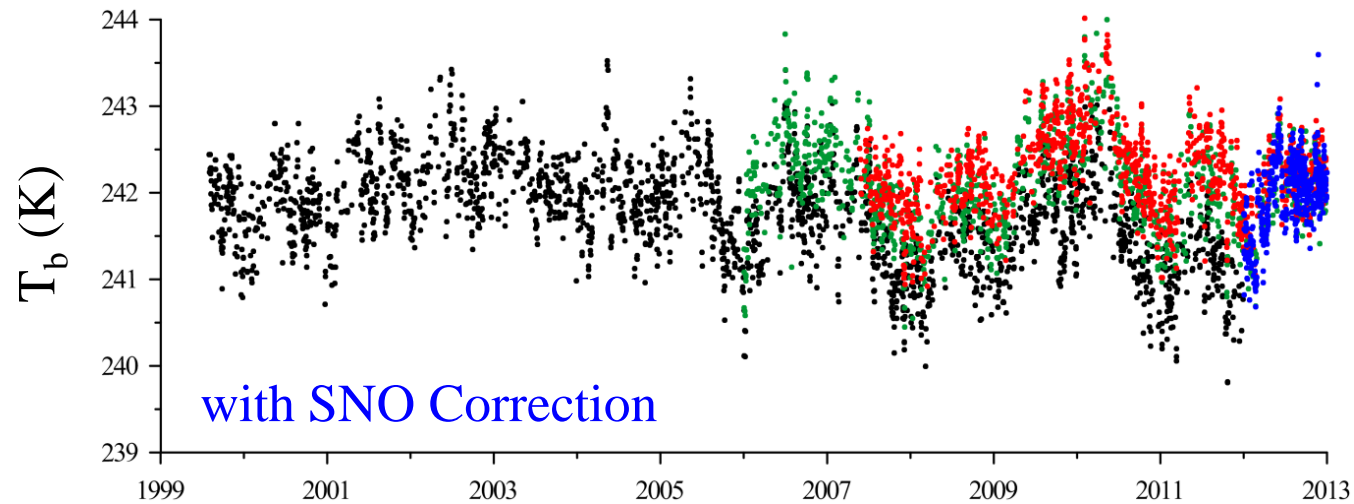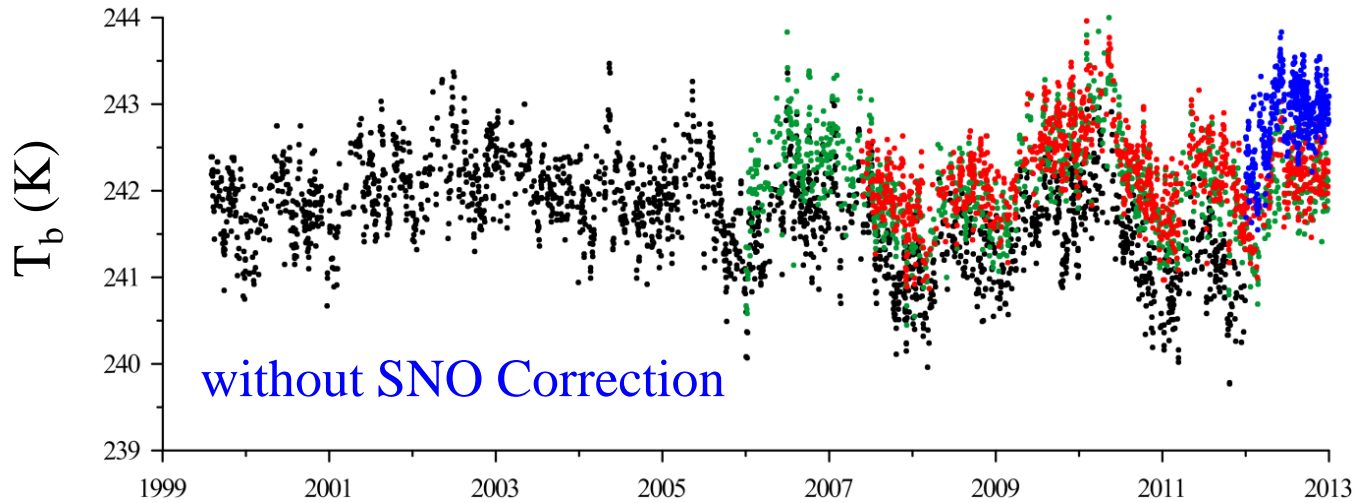
Data from NOAA-15, NOAA-18, MetOp-A, SNPP

Channel 6

Channel 7

before

before

after

after
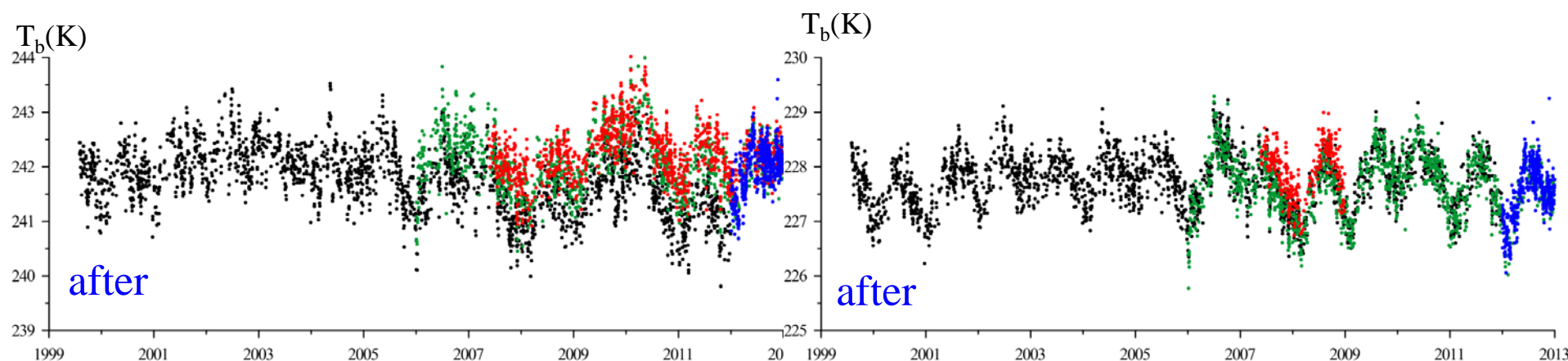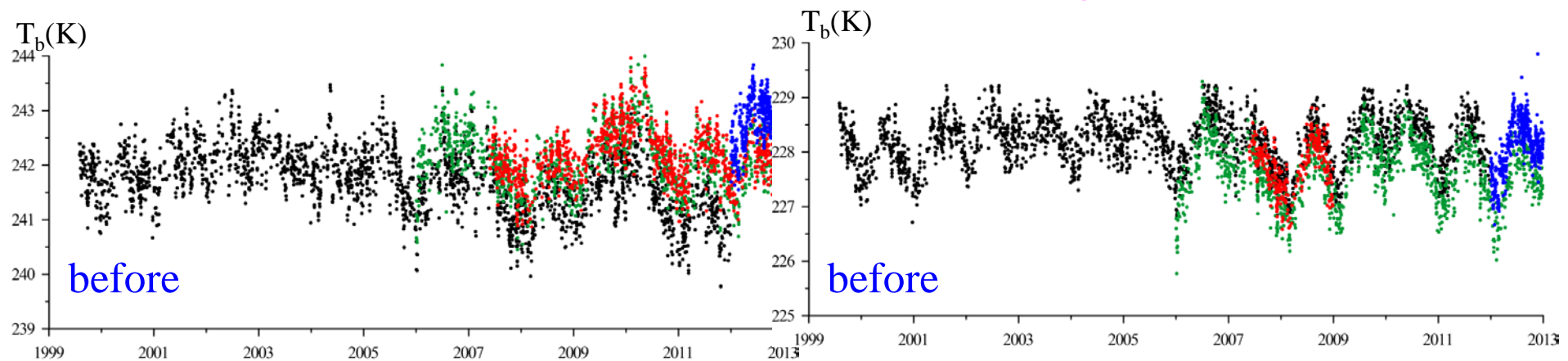
Nadir only, clear-sky, (2S-2N), (80W-180W)

Biases in the Tropics (NOAA-15, NOAA-18, MetOp-A, SNPP)
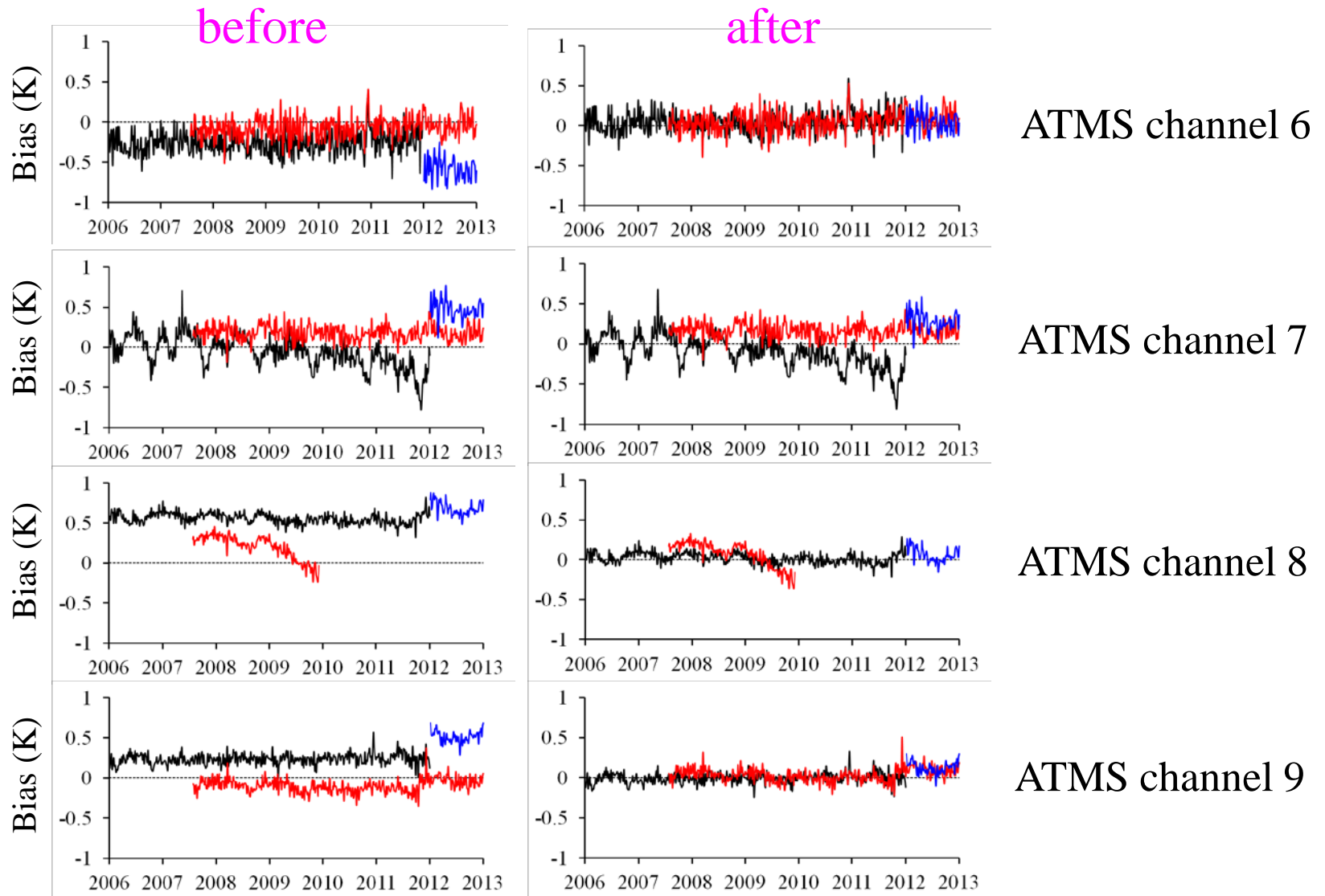
before   after

ATMS channel 6

ATMS channel 7

ATMS channel 8

ATMS channel 9

NOAA-18 is subtracted. The pentad data set within ±30° latitudinal band.

31

Biases in the Tropics (NOAA-15, MetOp-A, SNPP)

before   after

ATMS channel 10

ATMS channel 11

ATMS channel 13

ATMS channel 14
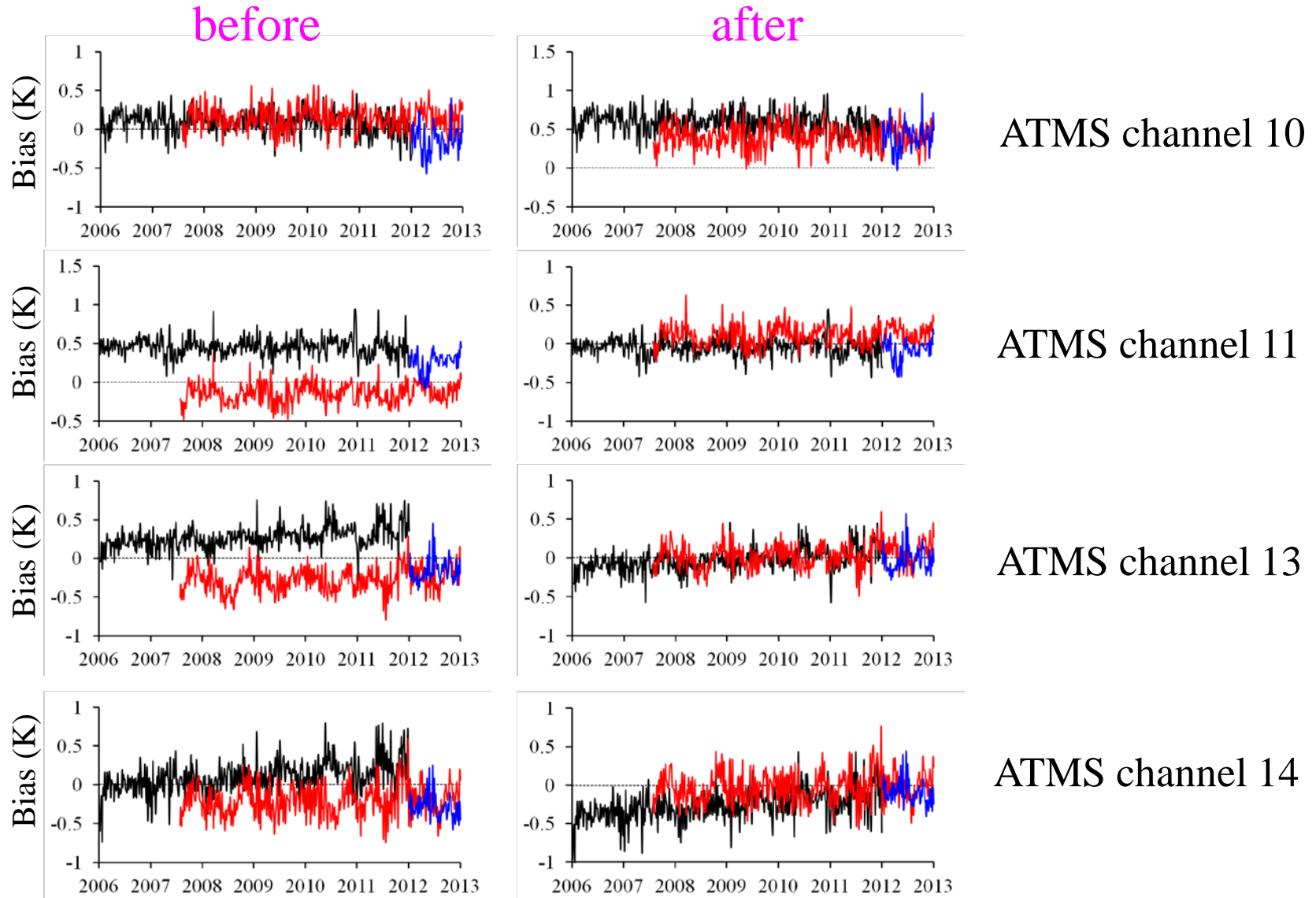
NOAA-18 is subtracted. The pentad data set within ±30° latitudinal band.

New Analysis of Atmospheric Temperature Trend from MSU and AMSU through non-Linear Trending

Ensemble Empirical Model Decomposition (EEMD)
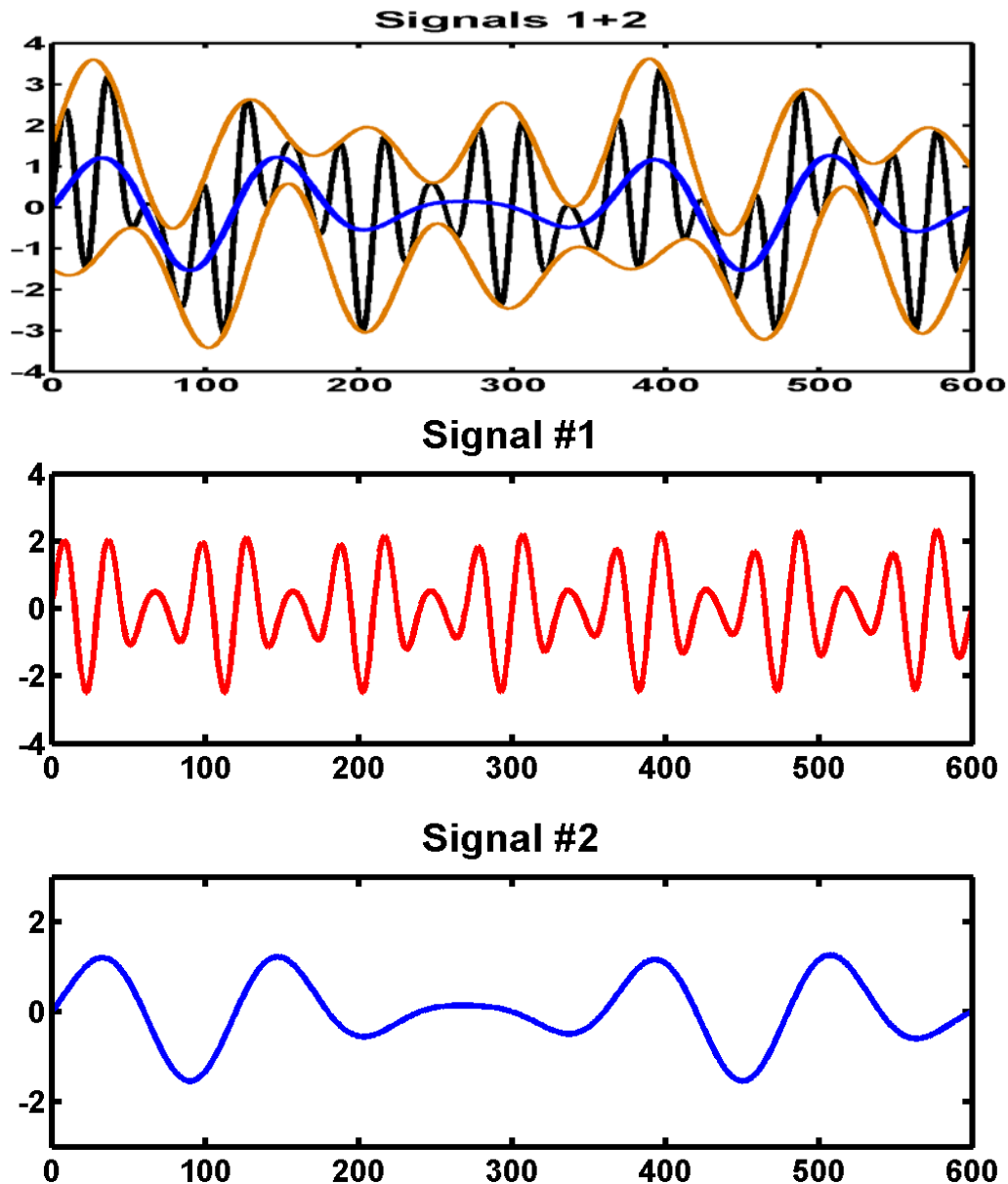
(Huang and Wu, 2008
Wu and Huang, 2009)

Advantage of EEMD over Linear Regression

- Work for waves of high and low frequency naturally mixing together

- No need to introduce *a priori* bases as used in Fourier transform or wavelet decomposition

- The separation of waves in this method is adaptive to data and is temporally local

- Climate trend is derived from the lowest frequency component

- The nonlinear trend is determined with less impacts by the data record length

NOAA-15 AMSU-A Channel 3 (50.3 GHz, surface)

Global average T_b
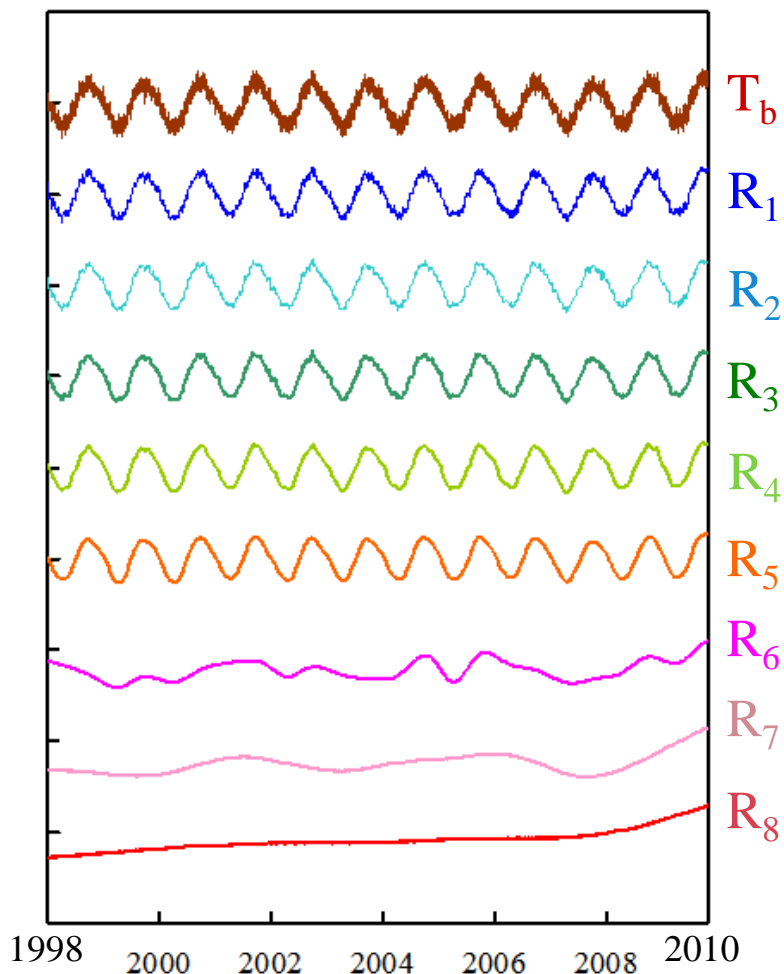
EEMD components
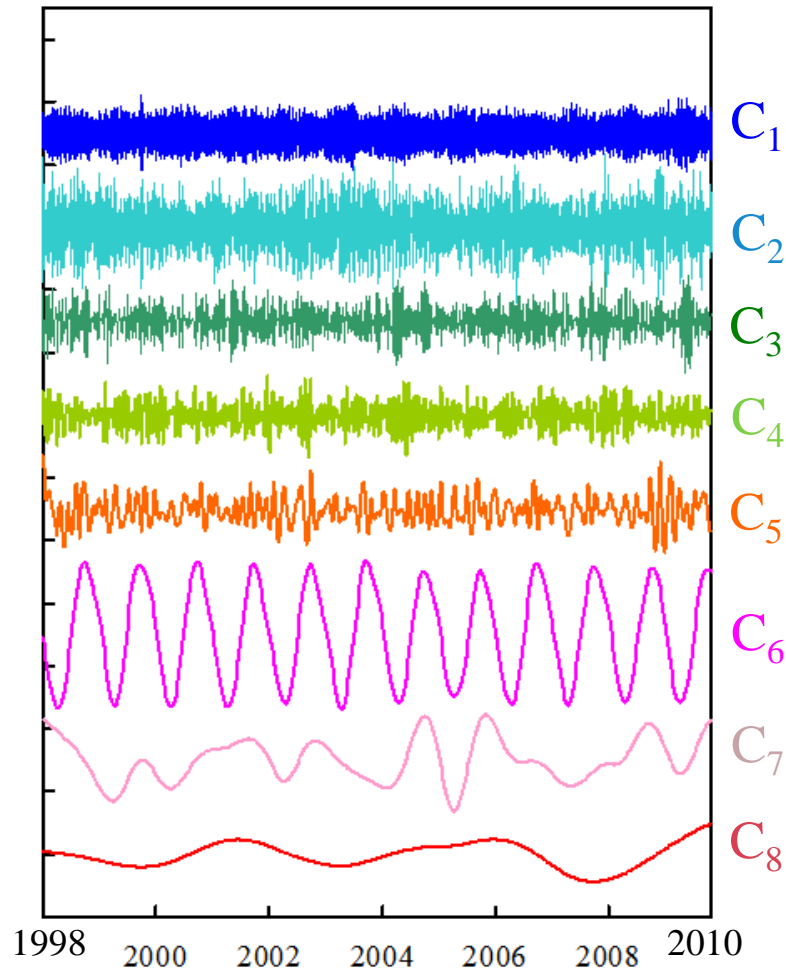
EEMD: $\overline{T}_b(t) = \sum_{j=1}^{n} C_j(t) + R_n(t)$ $R_n(t) = R_{n-1}(t) - C_{n-1}$
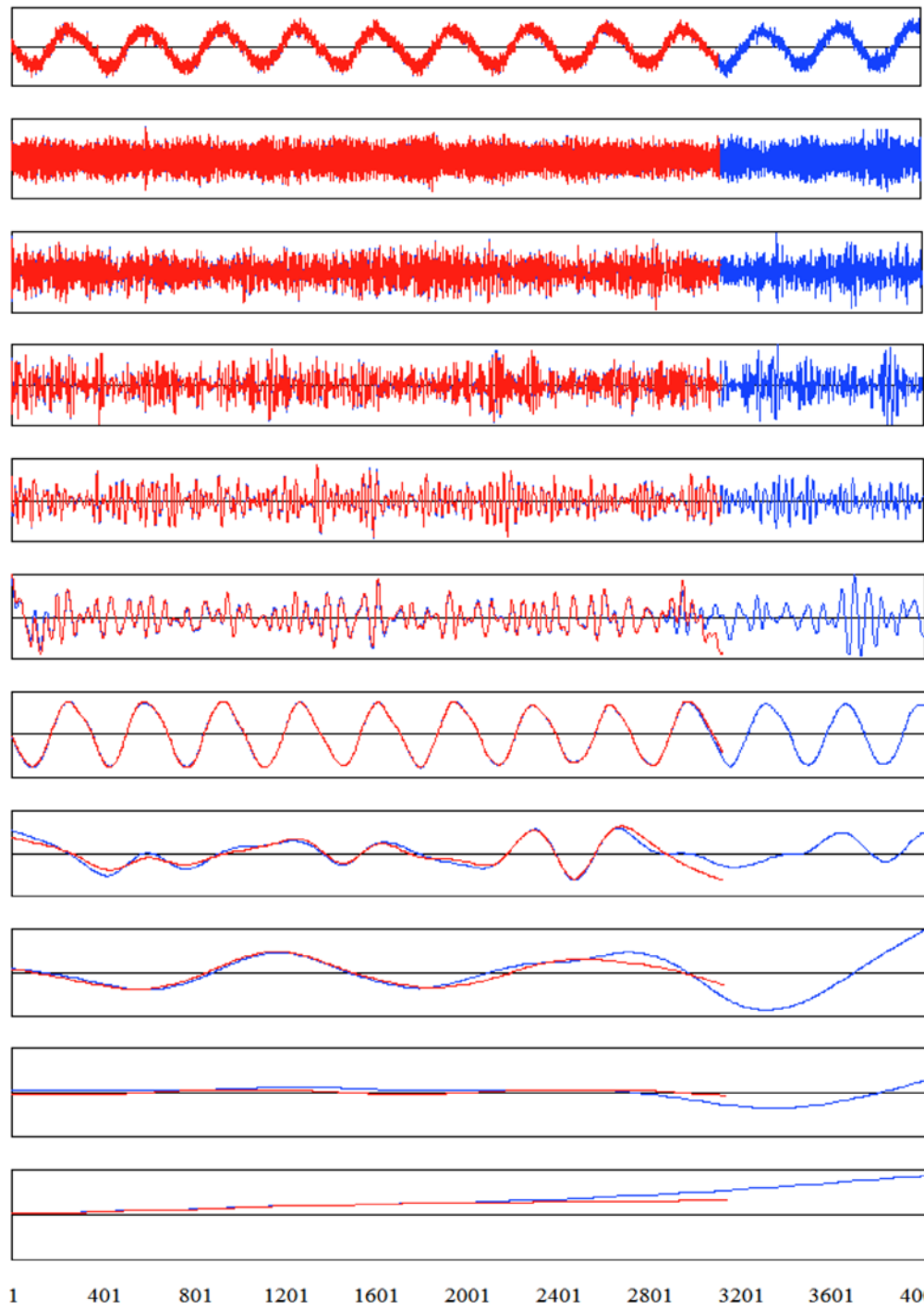
Raw radiance data

1st IMF

2nd IMF

3rd IMF

4th IMF

5th IMF

6th IMF

7th IMF

8th IMF

9th IMF

Trend

EEMD

13 years:
October 26, 1998
↓
August 7, 2010

11 years:
October 26, 1998
↓
December 31, 2008

(day)

37

NOAA-15 AMSU-A Channel 5 (53.596 GHz, 700 hPa)

Global daily mean T_b

Annual variation

EEMD trend

Linear trend
0.219 K/decade
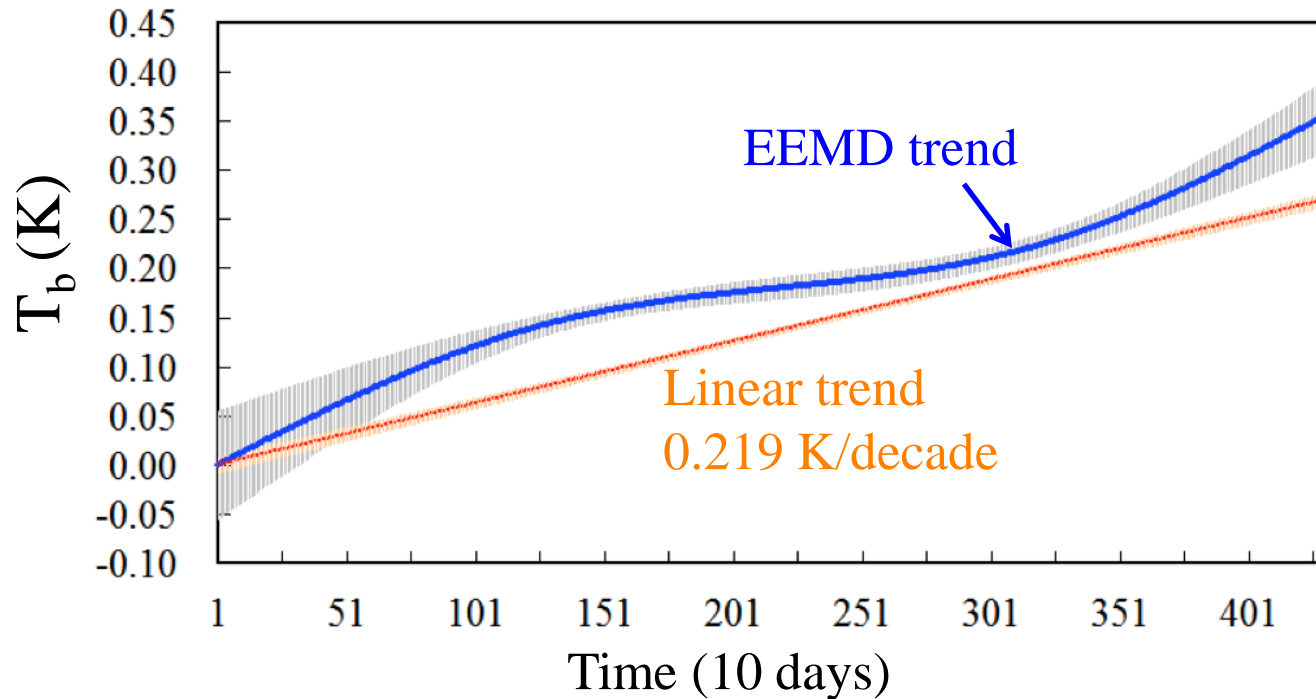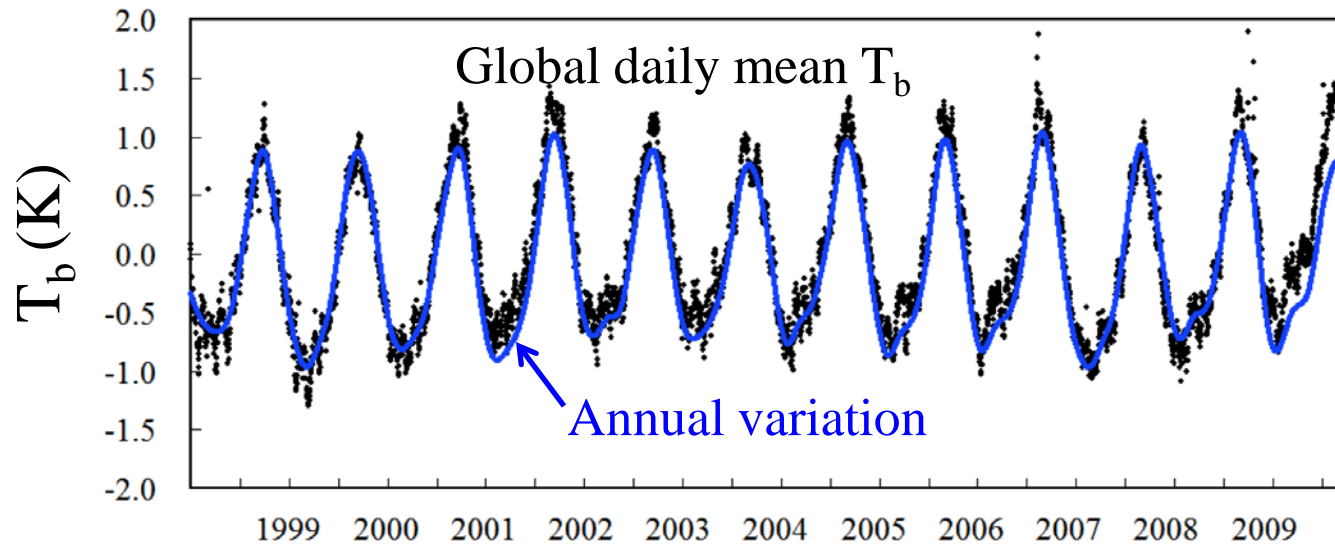
One data point
per 10 days
50 members

Time (10 days)

38

Climate Trend Derived by EEMD Method
for All AMSU-A Channels on NOAA-15
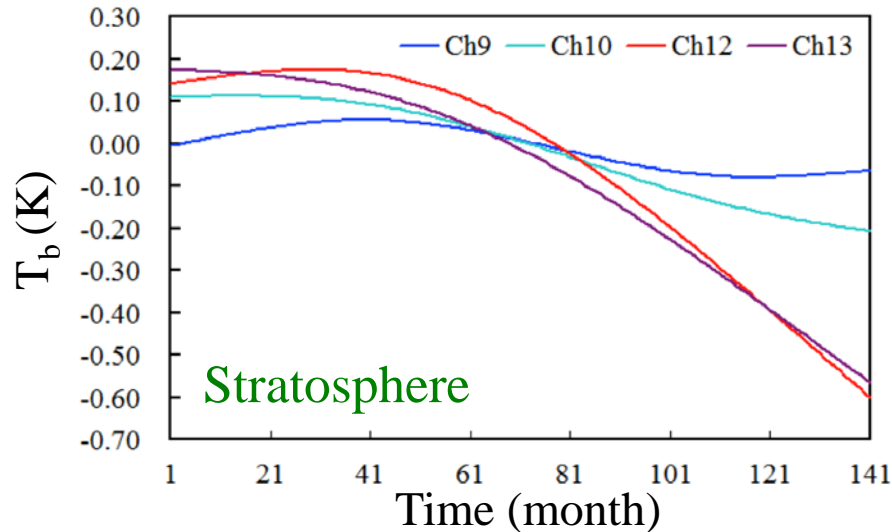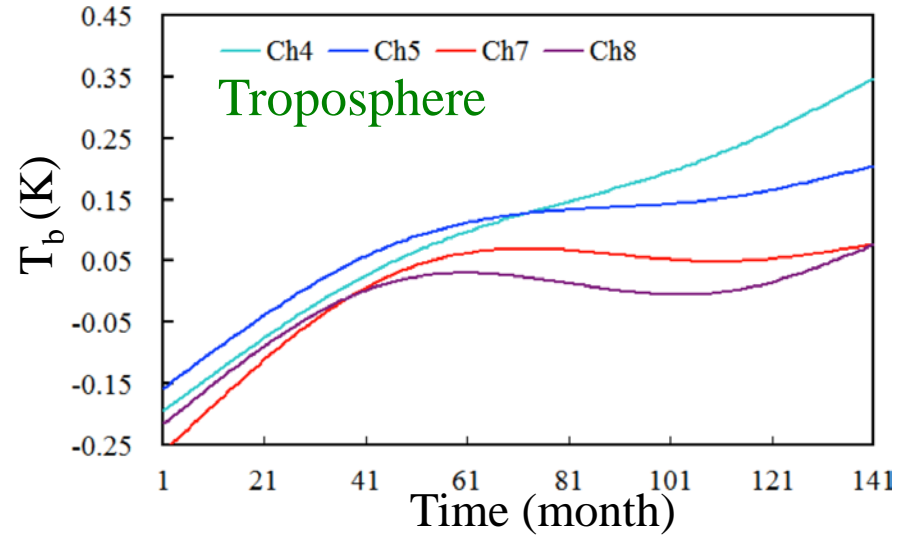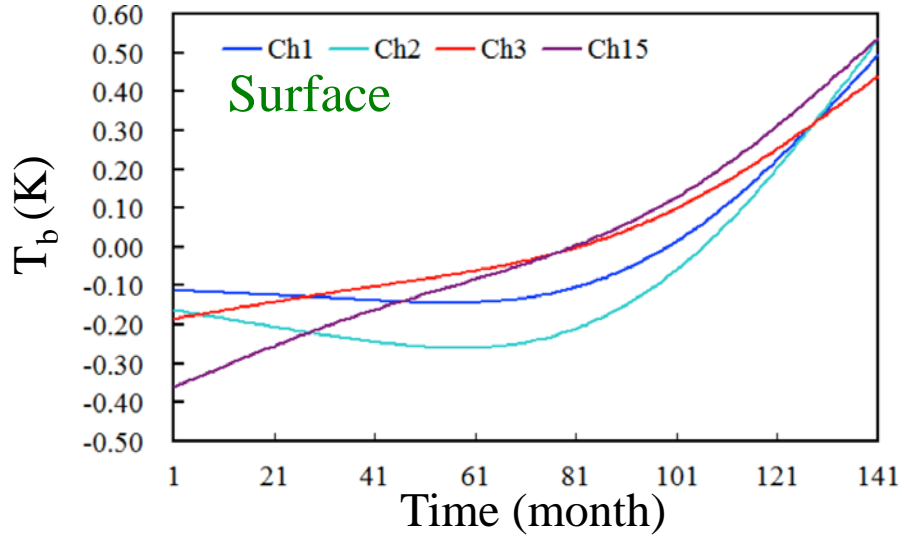
Atmospheric Temperature Trends from NOAA-15 AMSU-A Clear-Sky only Data
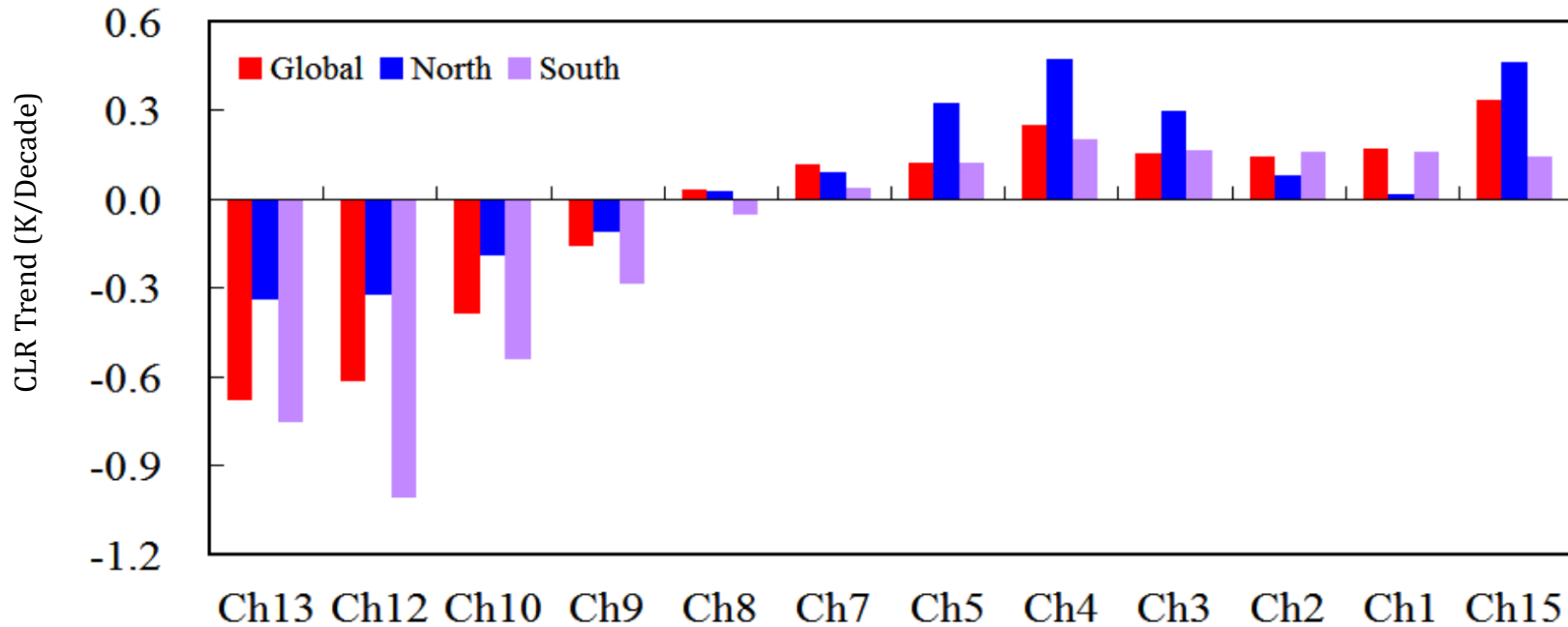
 Global (red), Northern Hemispheric (blue) and Southern Hemispheric (purple) warming and cooling trends of daily mean brightness temperatures of 12 AMSU-A channels of NOAA-15 calculated by the CLR method from 13 years brightness temperature measurements.

Contribution of Regional Climate Trend on Global Mean using Regression Mode

The following formula is used to derive the regressed trend from both the traditional linear regression and EEMD methods:

$$R(\lambda,\varphi) = \frac{\sum_{i=1}^{141}\left(T_b^{\text{linear evolution}}(t_i) - \sum_{i=1}^{141} T_b^{\text{linear evolution}}(t_i)\right)\left(T_b(\lambda,\varphi,t_i) - \sum_{i=1}^{141} T_b(\lambda,\varphi,t_i)\right)}{std(T_b)}$$

EEMD trend
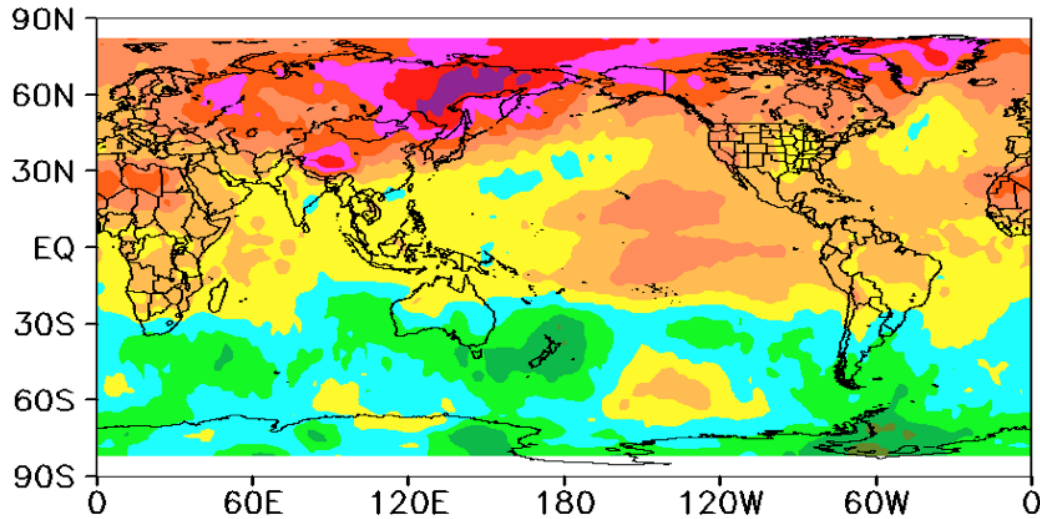
Contribution from each location to the total warming derived from regressed mode

Linear trend

Channel 5
(53.596 GHz, 700 hPa)

42

(0.1K)

EEMD trend

Contribution from each location to the total warming derived from regressed mode
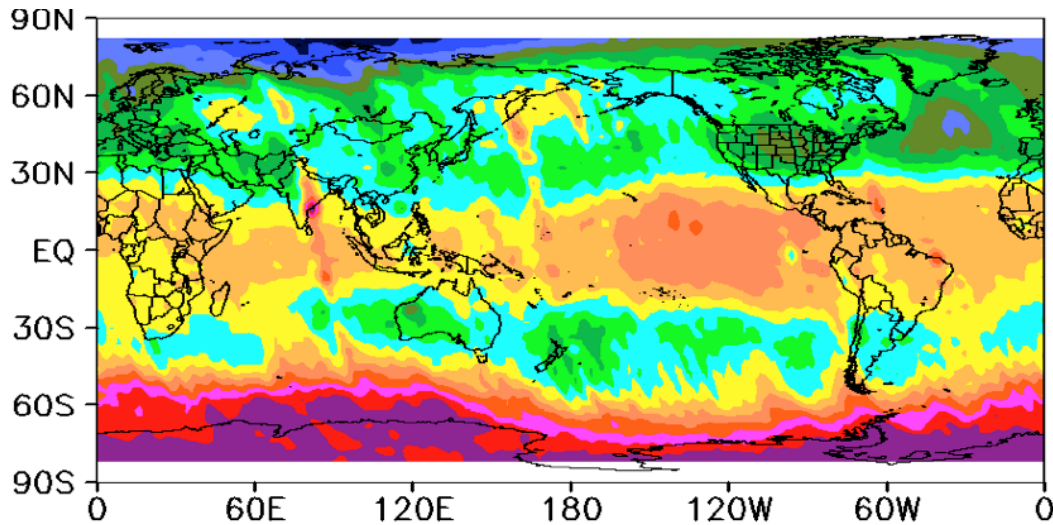
Channel 9
(57.29 GHz, 70 hPa)

Linear trend

(0.1K)
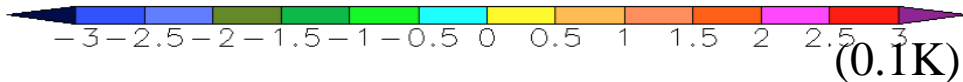
Global Linear Trend

Stratospheric (Top) and Tropospheric (bottom)
Channels in Northern Hemisphere
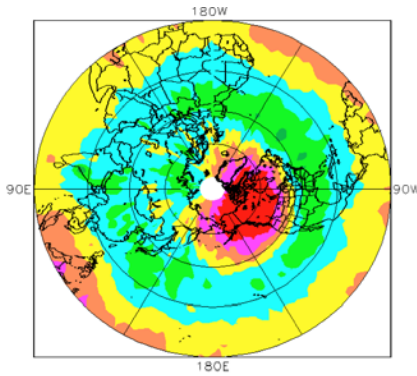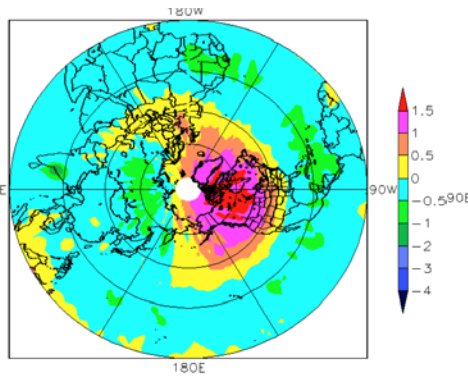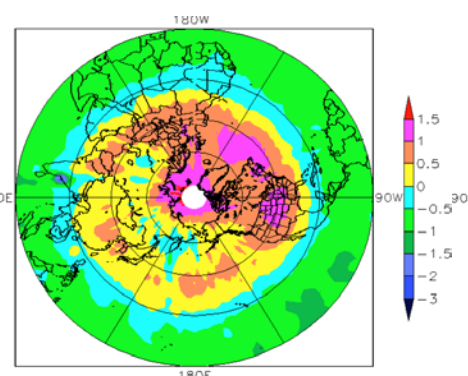
Ch13   Ch12   Ch10   Ch9
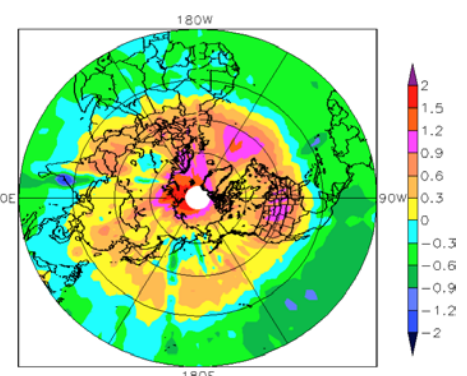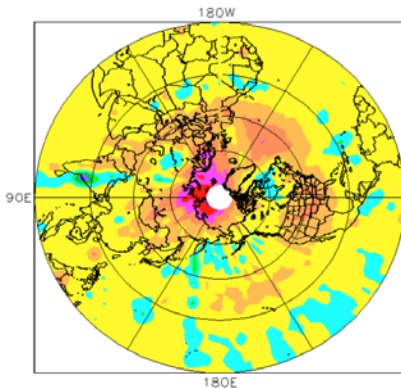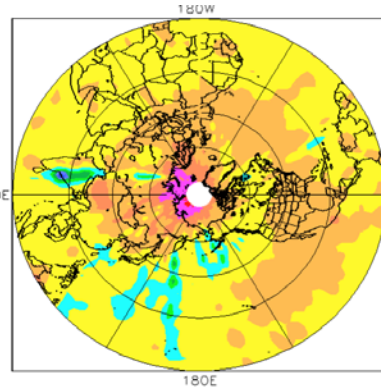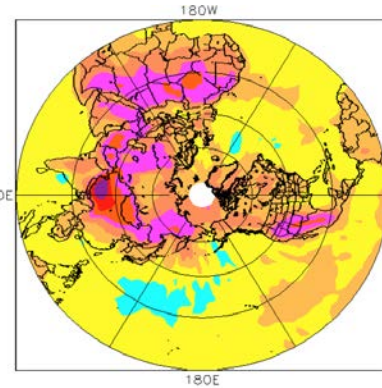
Ch8   Ch7   Ch5   Ch4
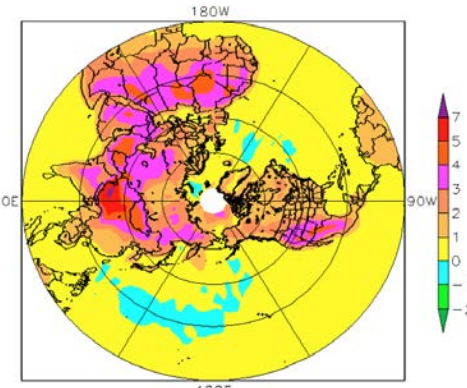
Tropospheric Channels in Northern Hemisphere

44
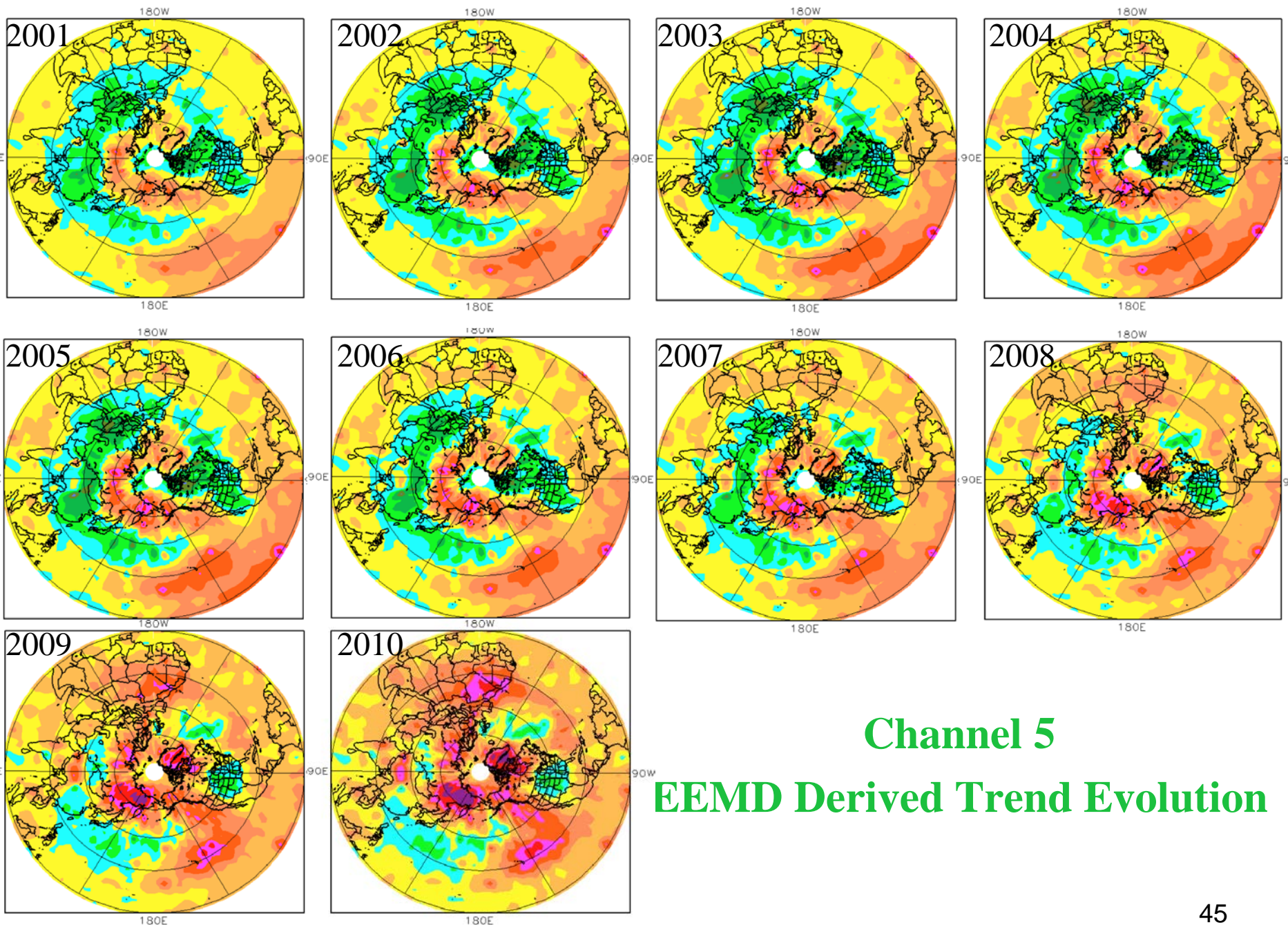
Channel 5
EEMD Derived Trend Evolution

45

2001   2002   2003   2004

2005   2006   2007   2008

2009   2010   Linear regression

−2 −1.5 −1.2 −0.9 −0.6 −0.3 0 0.3 0.6 0.9 1.2 1.5 2
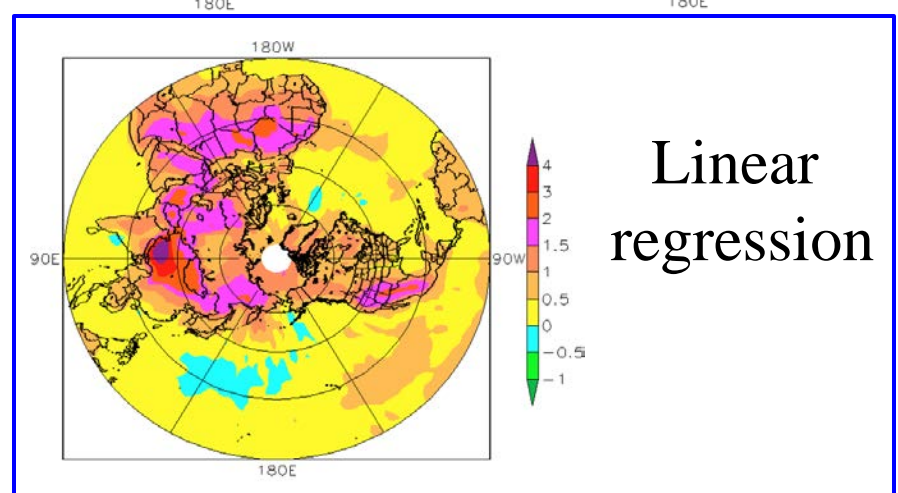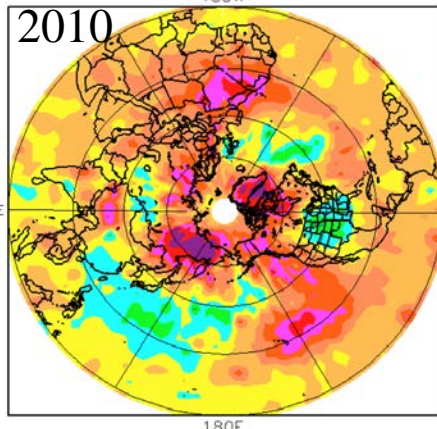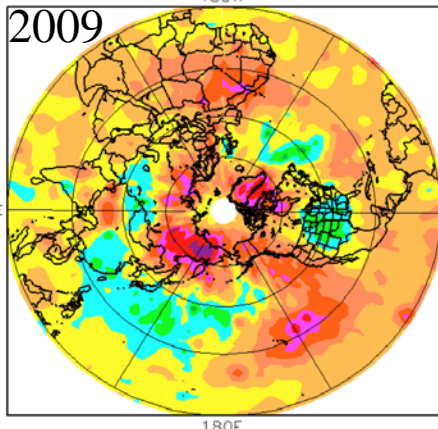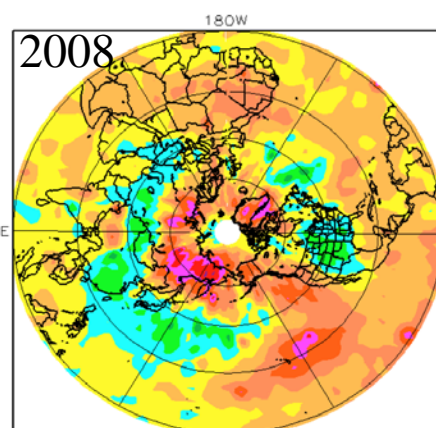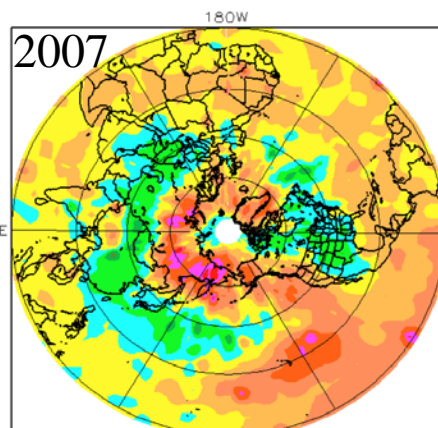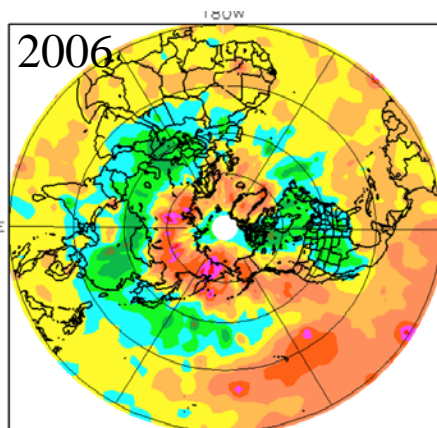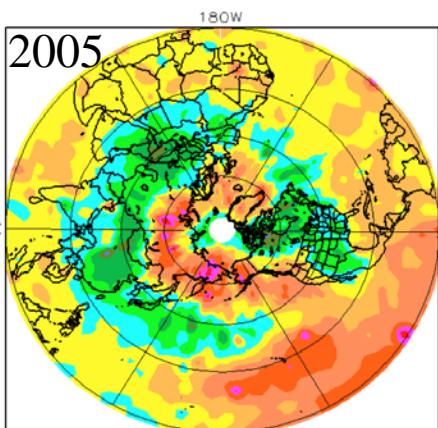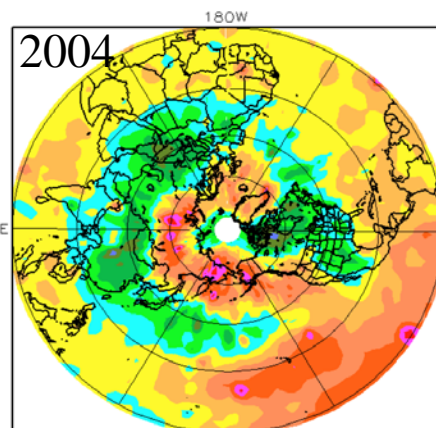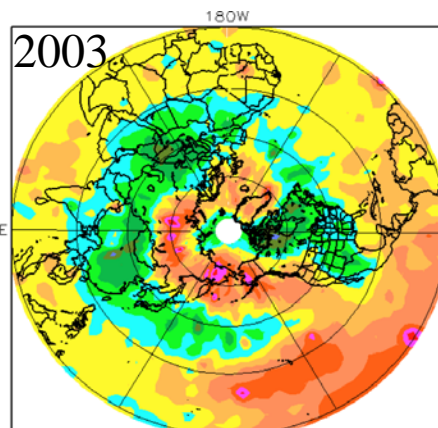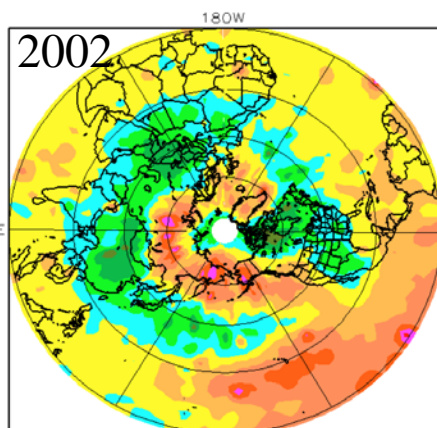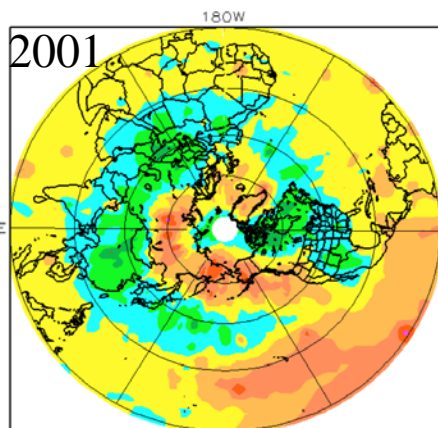
Updated time series of the annual mean surface temperature for 1900-2012 in China
最新的中国百年温度曲线
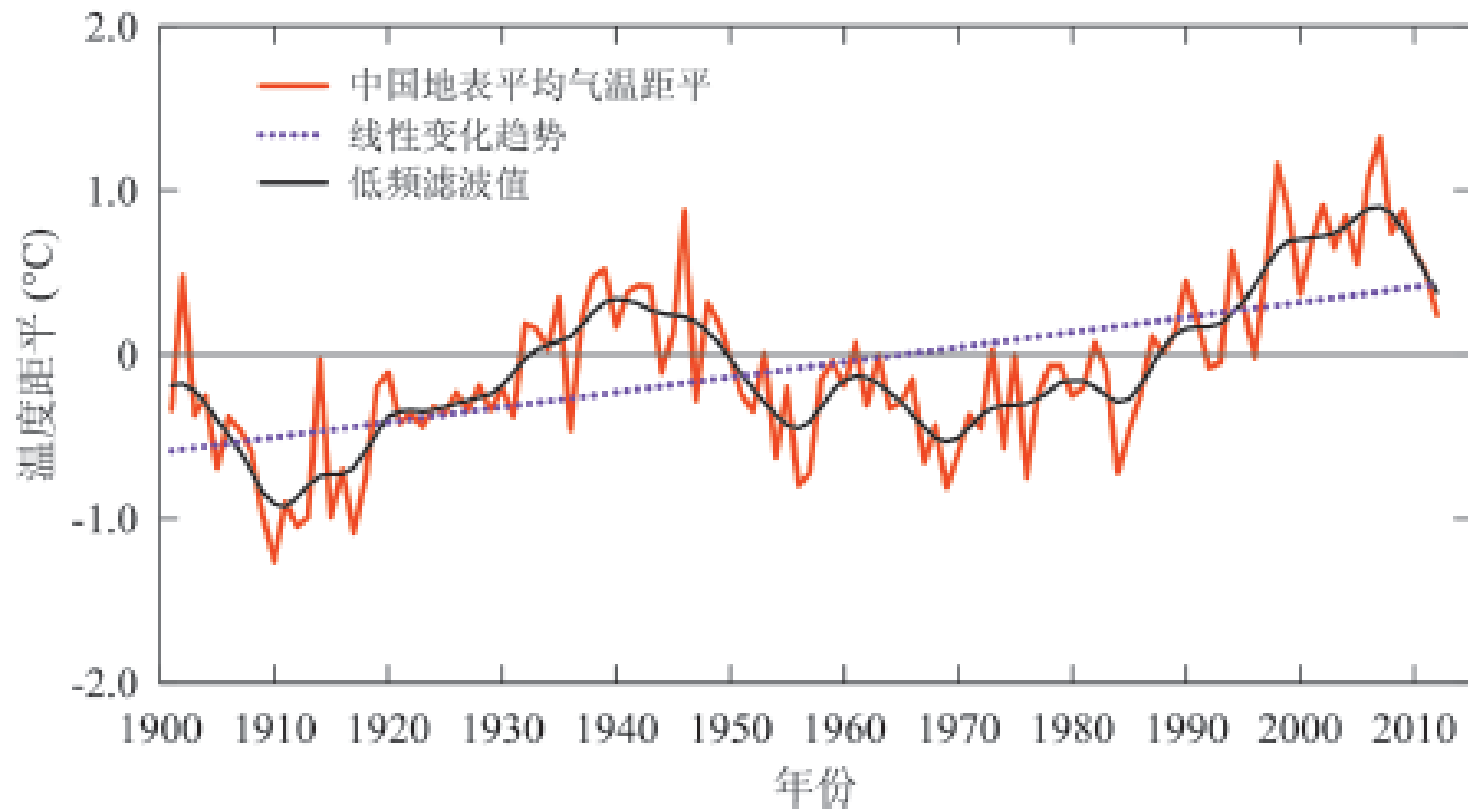
（Ding Yihui，2014）

Effects of Clouds and Precipitation on AMSU Derived Climate Trend

New Analysis of Atmospheric Temperature Trend from MSU and AMSU
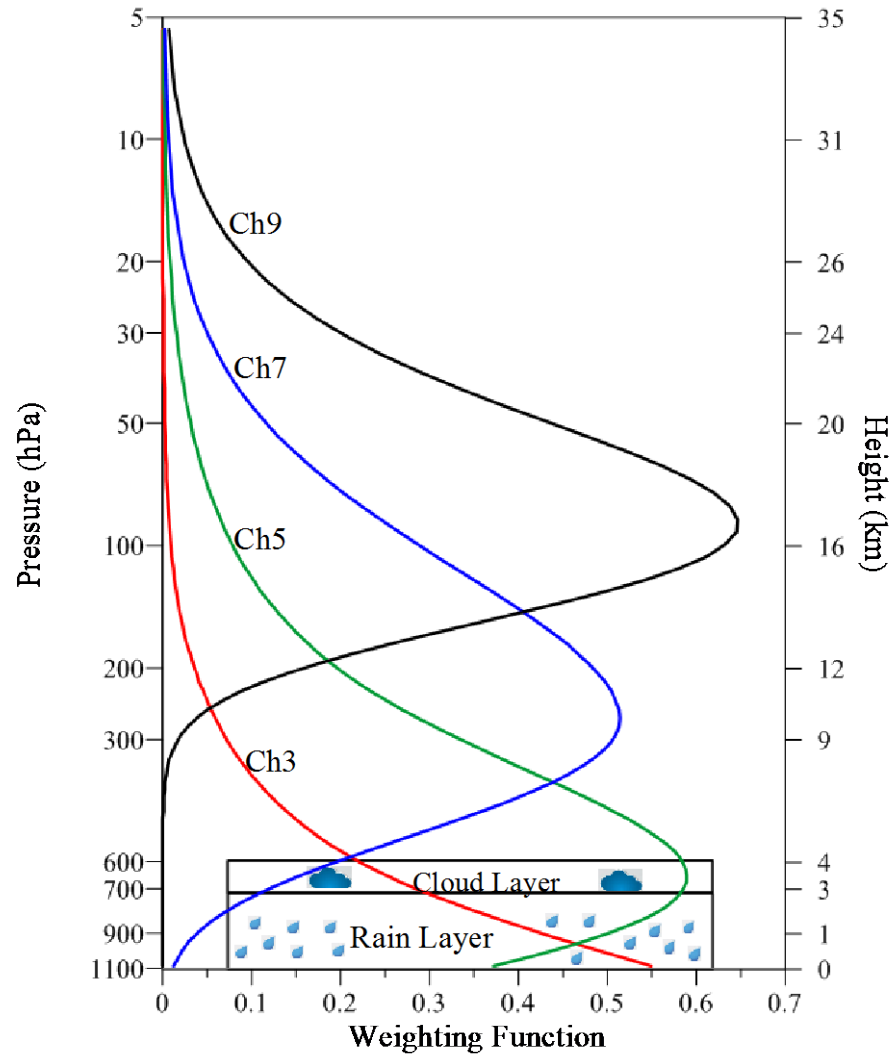
Cloud Effects on AMSU Brightness Temperature
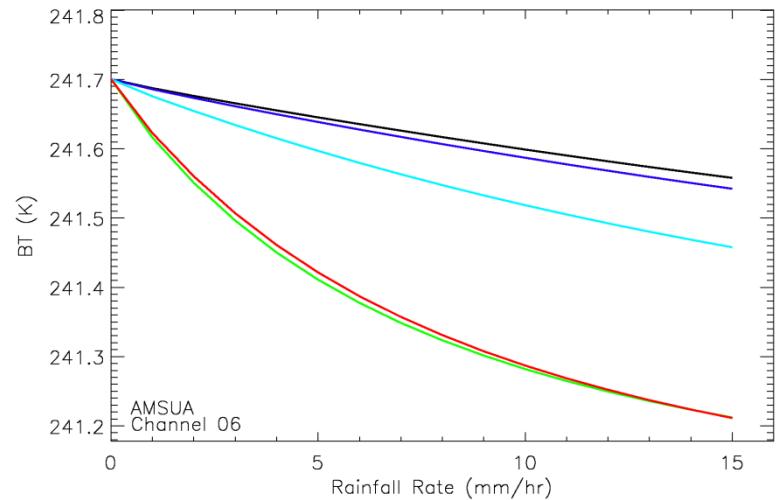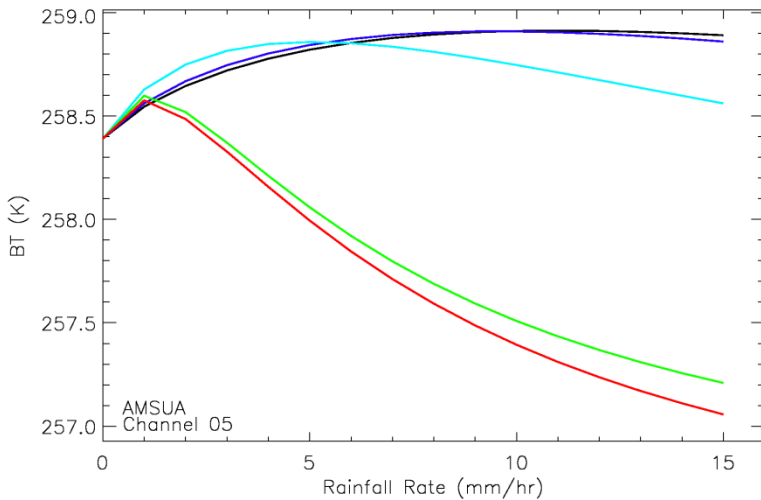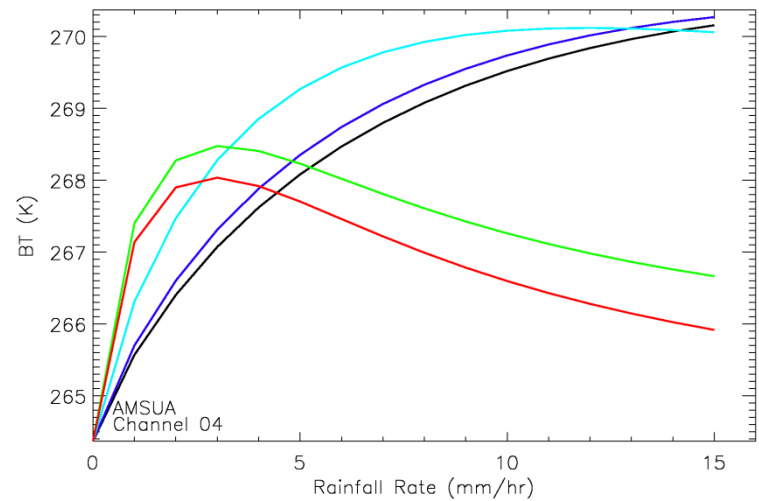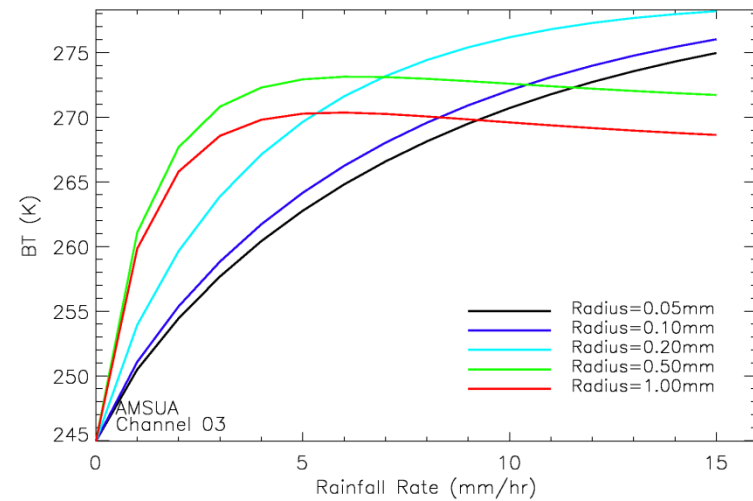
Assume a stratiform rainfall with intermediate rainfall rate: A cloud layer about 0.8 km depth below the freezing level with liquid water path of 0.5 kg/m2, and the raindrops all below the non-precipitating cloud layer and the rainfall rates unchanged vertically. Emissivity set to 0.5.

Population of AMSU-A Channel 5
Clear (red) and All Sky Measurements (blue)
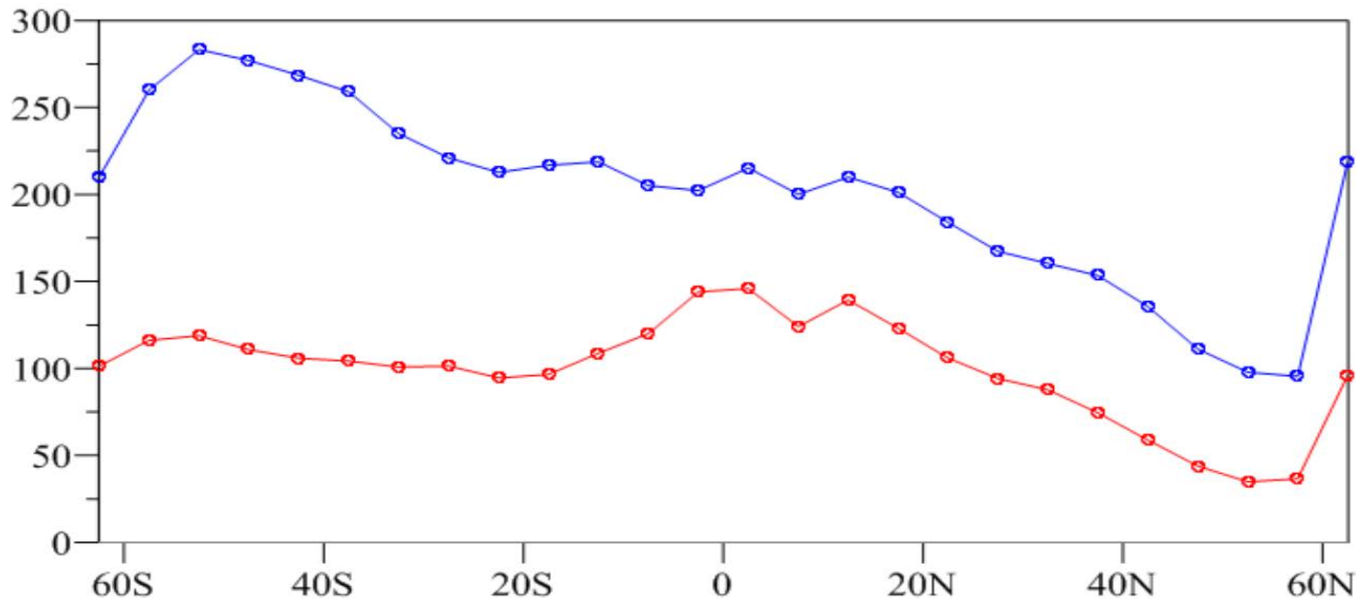
Annual mean daily data count at 5.0 degree resolution latitudinal band for NOAA-15 channel 5 FOV 15 and 16 in 2008 with LWP < 0.5 kg/m^2 (blue line) and LWP < 0.01 kg/m^2 (red line). All the AMSU data for the region north of 60N and 60S are included in the first and last point on the curve.

Cloud Impact on MSU/AMSU Derived Trends
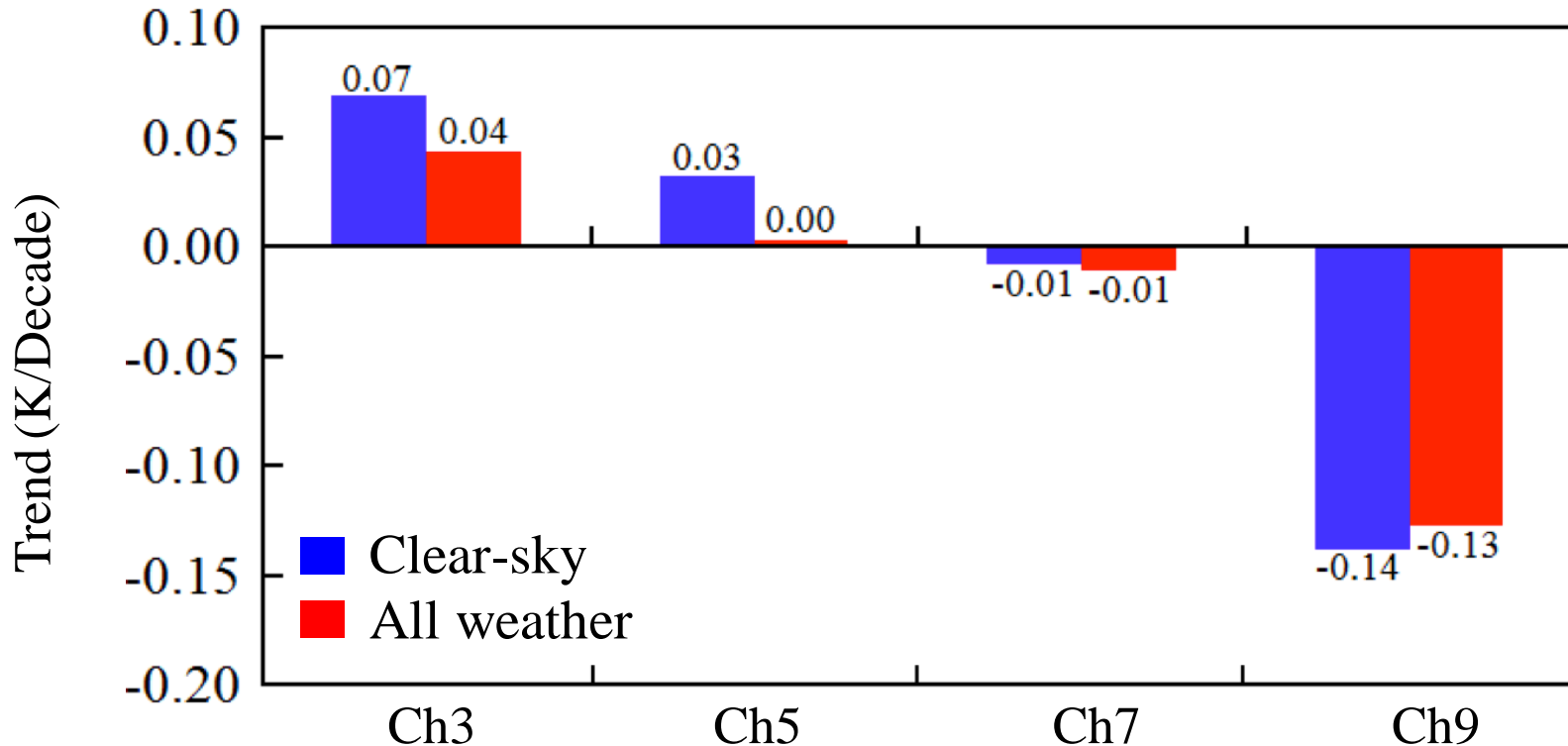
Weng, F. X. Zou and Z. Qin, 2013: Uncertainty of AMSU-A derived temperature trends in relationship with clouds and precipitation. *Clim. Dyn.*, DOI 10.1007/ s00382-013-1958-7.

Cloud Impacts on MSU/AMSU Channel 5 Derived Trends in South and North Hemispheres
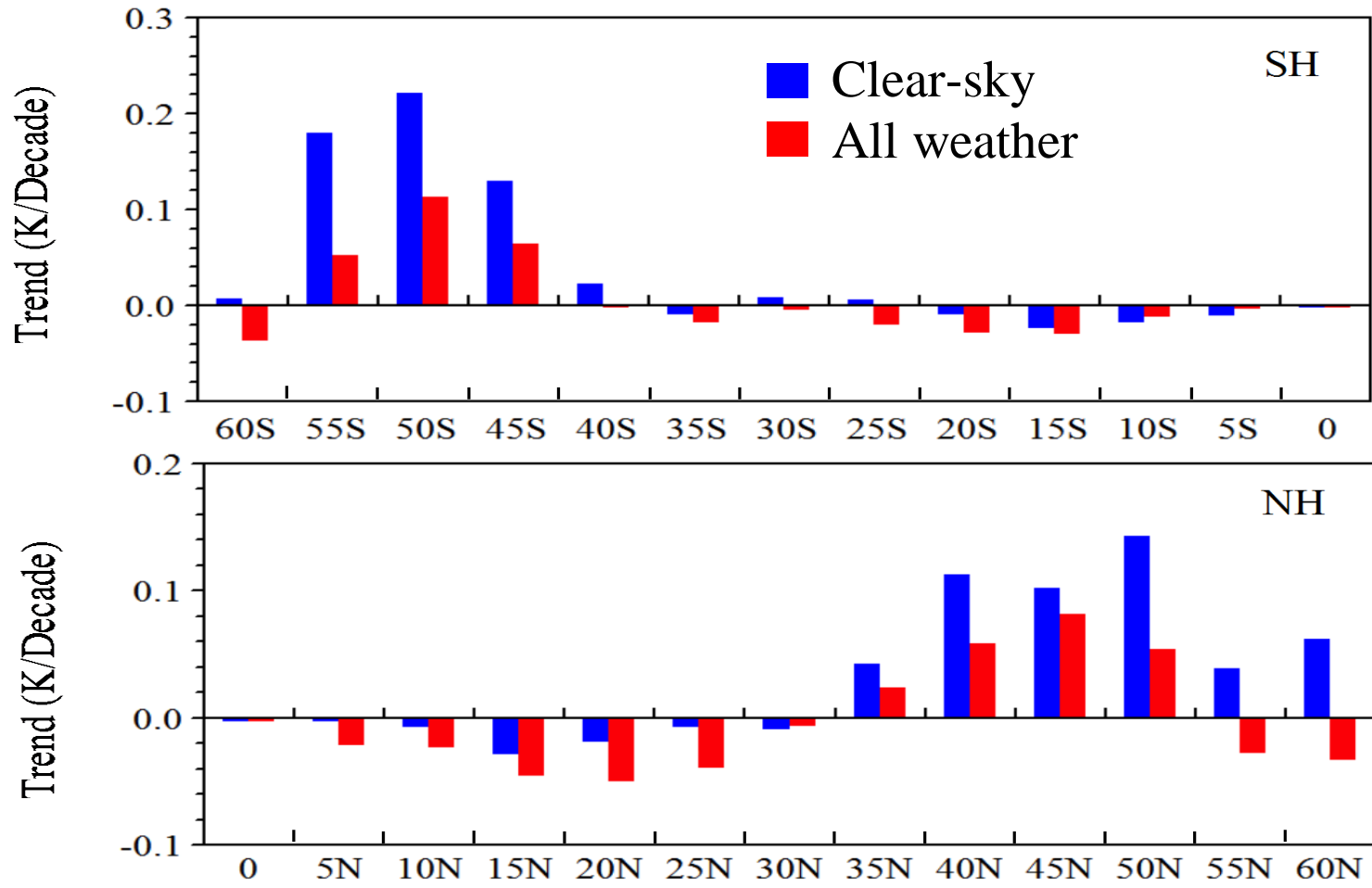
Regional Contribution to the Global Trend from Clear-Sky and All Weather AMSU-A Data
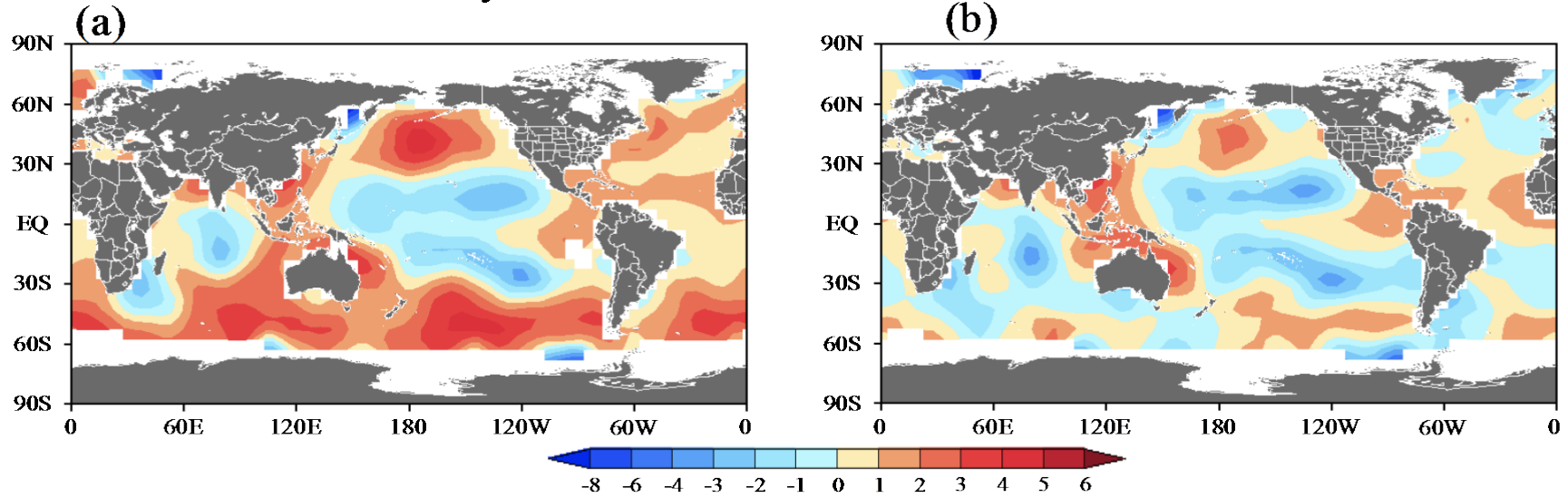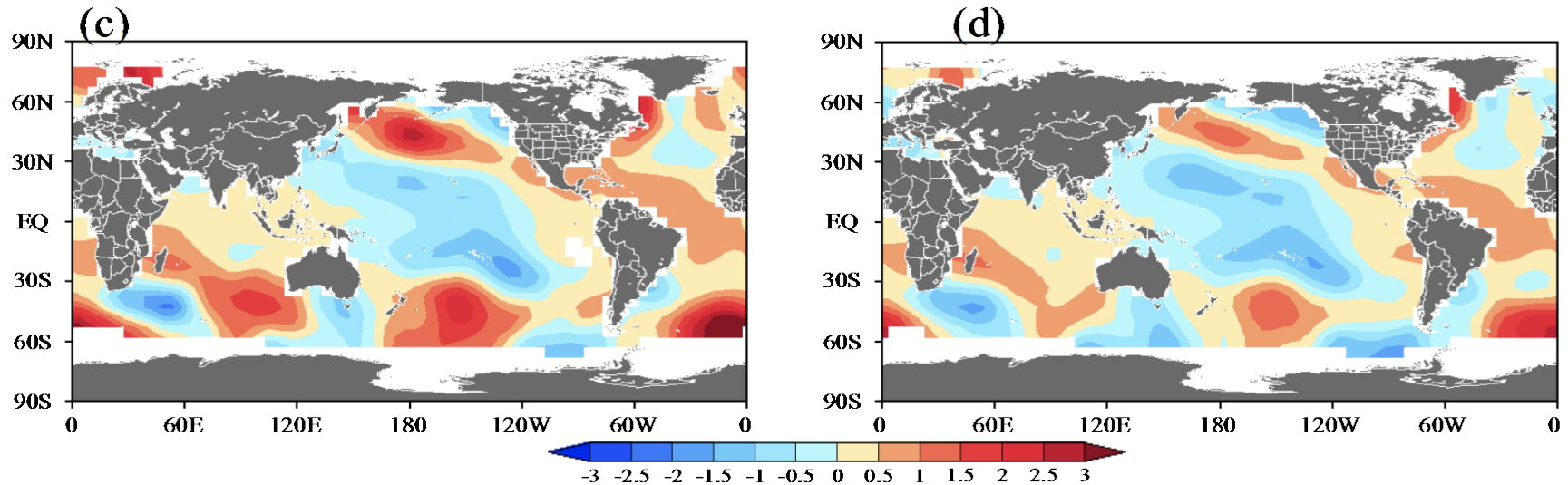
Temperature Trend from 1DVAR Retrievals

One-Dimension Variational Retrieval
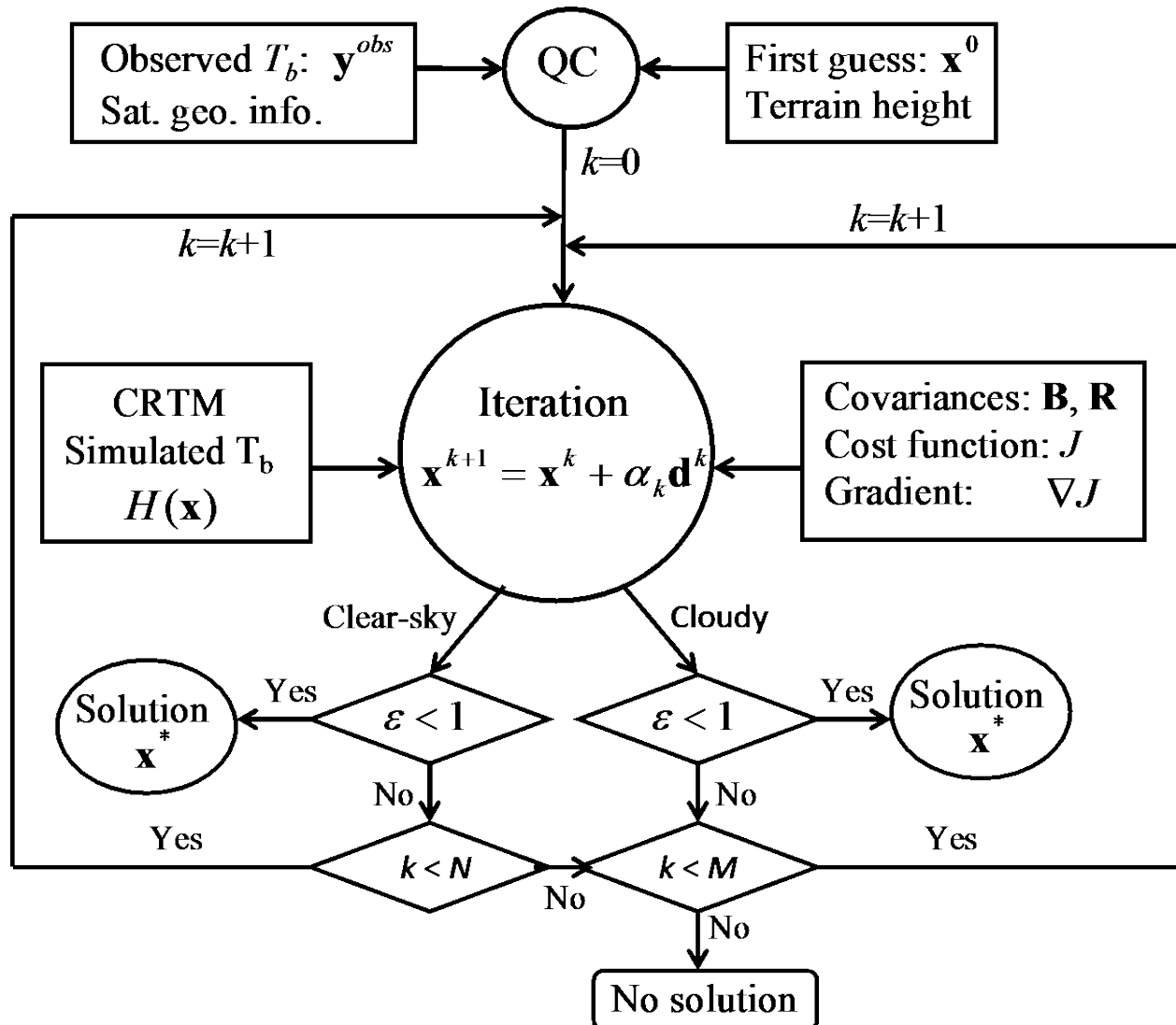
Uses of MSU Channel 1 and 2 for Cloud Detection
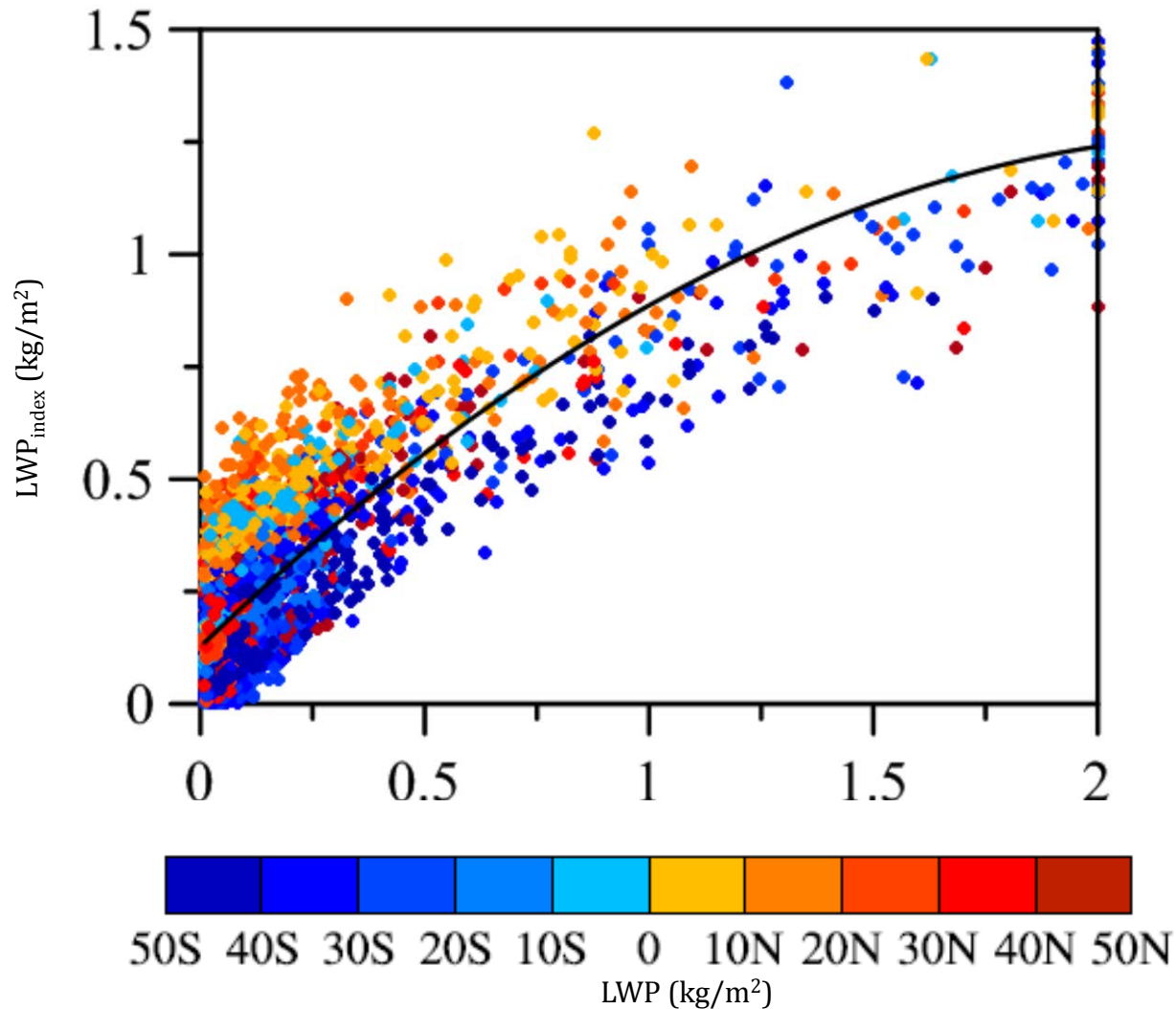
Detection of Clouds from MSU like Instruments
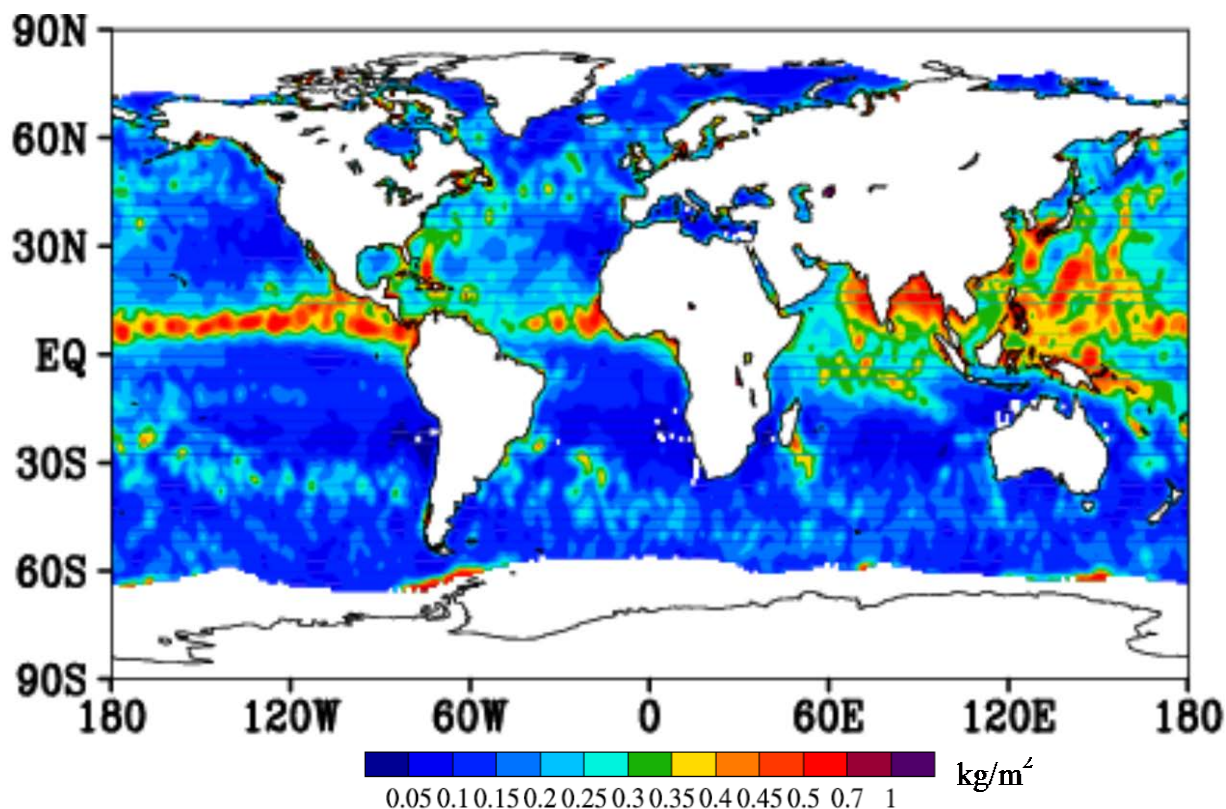
Scatter plot of LWP index derived from MSU-like AMSU-A channels 3 and 5 using equation (4) (y-axis) and LWP derived from AMSU-A channels 1 and 2 for nadir only over ocean on August 1, 2011. The black line represents a parabolic fitting: LWP_{index}= -0.16*LWP^2 + 0.87*LWP+0.15. (b) Global distribution of monthly mean cloud LWP_{index} (unit: kg/m²) within 1º × 1º grid box over ocean in August 2011.

Error Profiles from MSU Temperature Retrieval as Compared with GPSRO Data
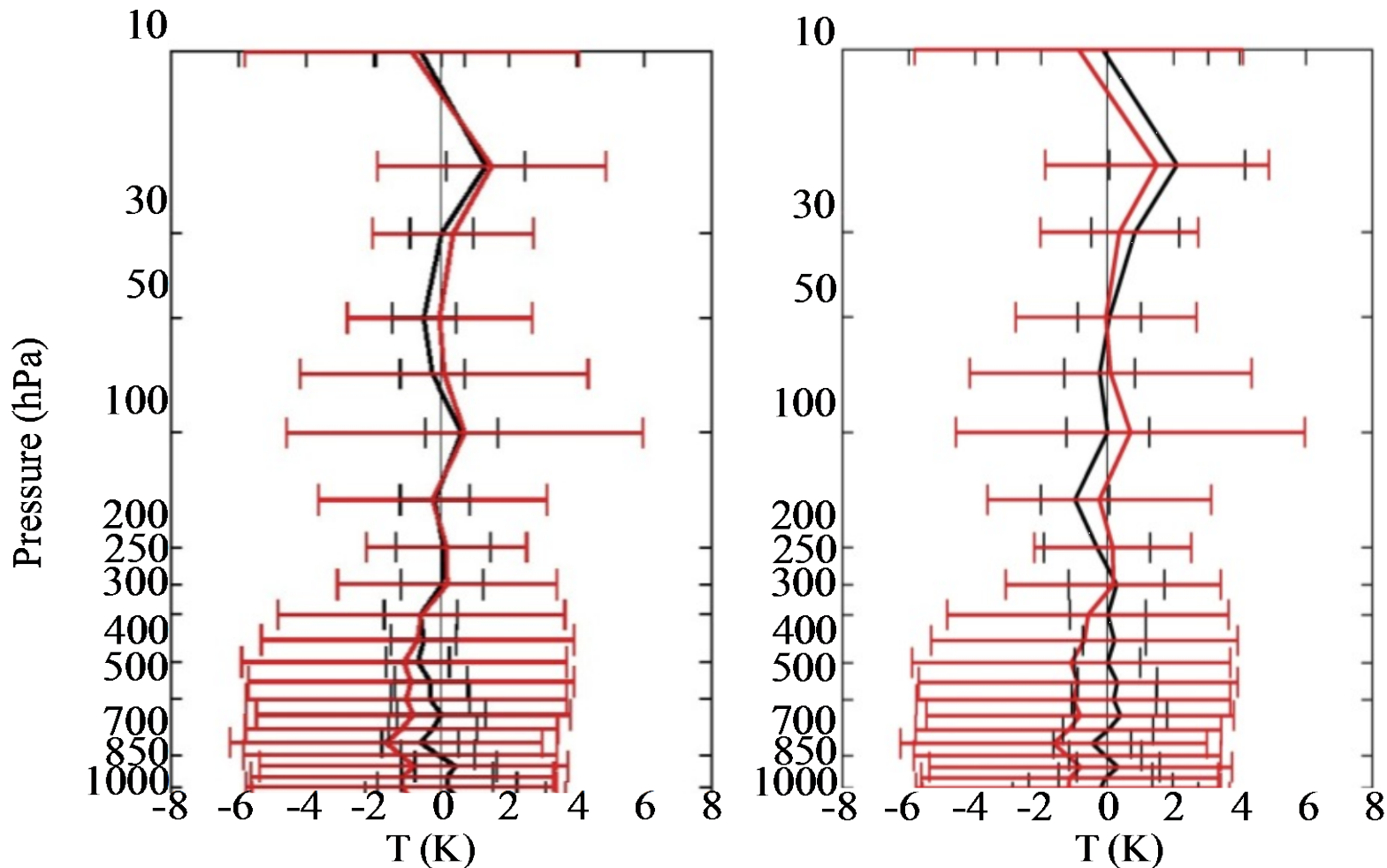
Mean error (solid) and RMS errors (horizontal bar) of atmospheric temperature profiles from the initial guess (red) and the 1D-Var retrievals (black) verified with COSMIC GPS RO data during June 1-10 in 2008-2011. Collocation criteria in time and space are set to be one hour and 50 km, respectively. (a) Only AMSU-A channels 3, 5, 7 and 9 are assimilated. (b) All AMSU-A channels are assimilated

Mean Temperature Trends from 1990 to 2010 at Different Pressure Levels
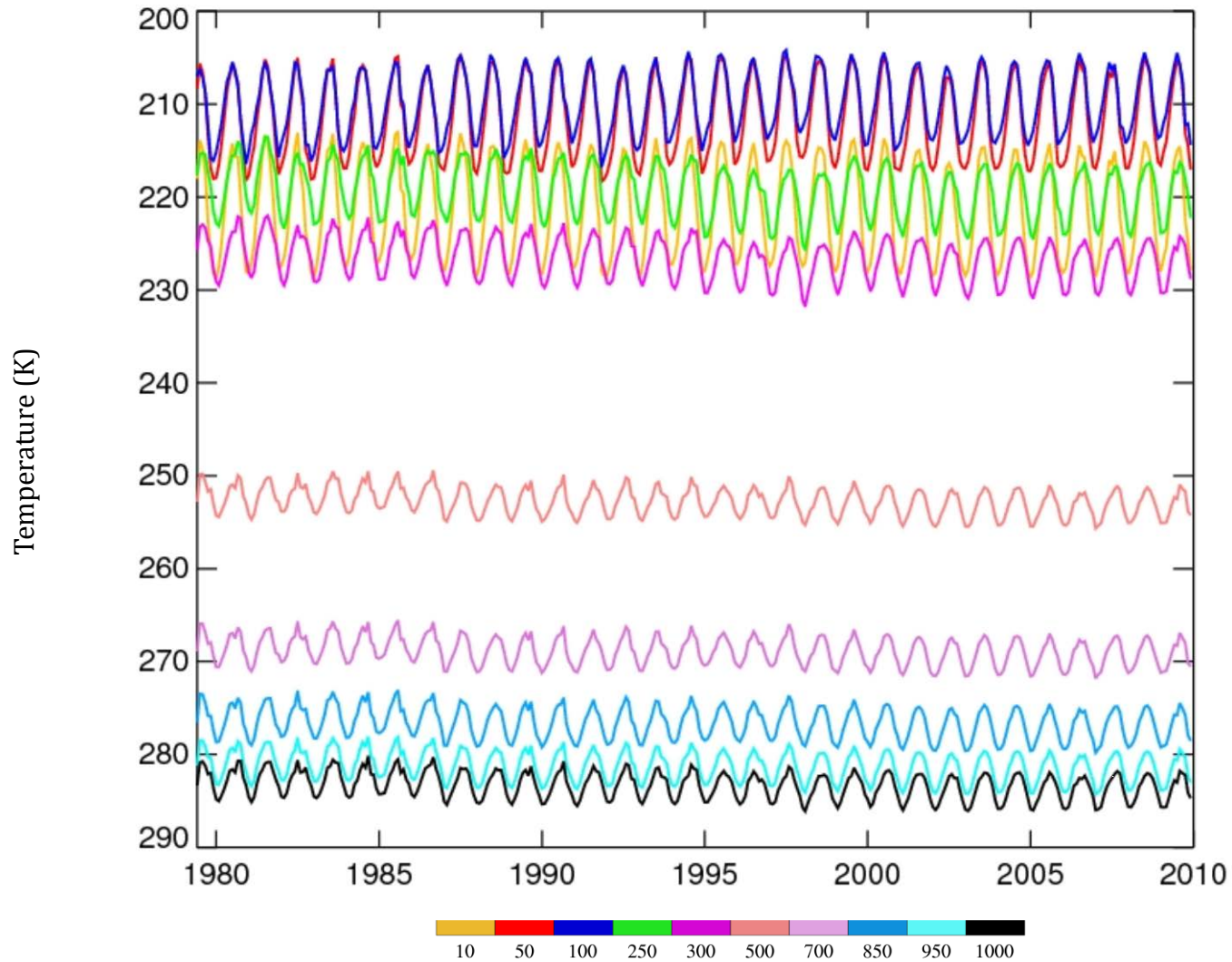
Mean Temperature Trends from 1990 to 2010 at Different Pressure Levels (1/3)
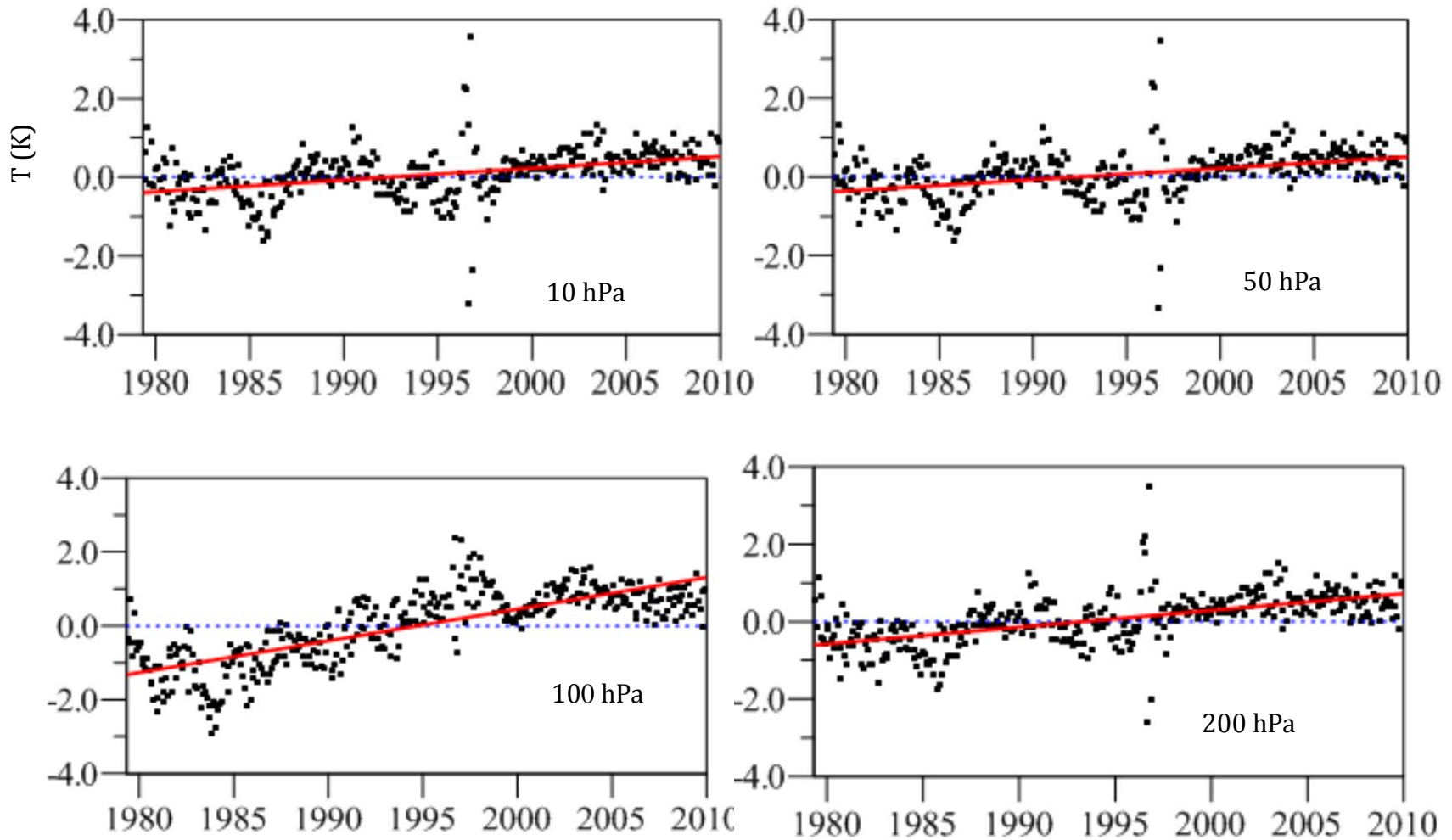
Mean Temperature Trends from 1990 to 2010 at Different Pressure Levels (2/3)
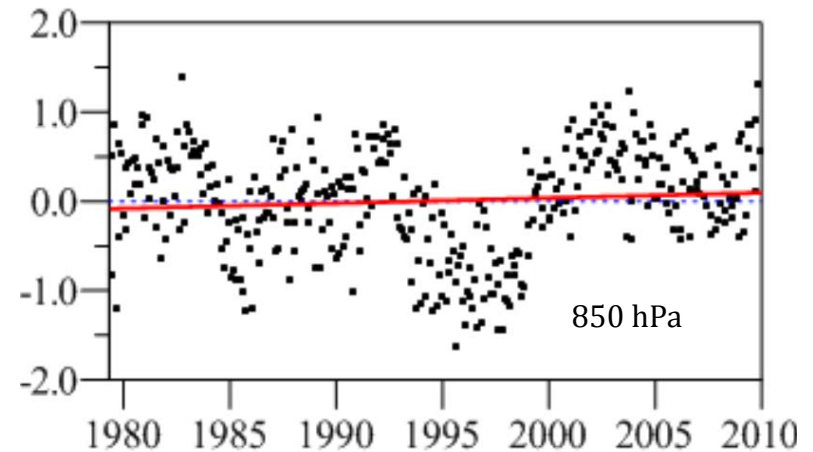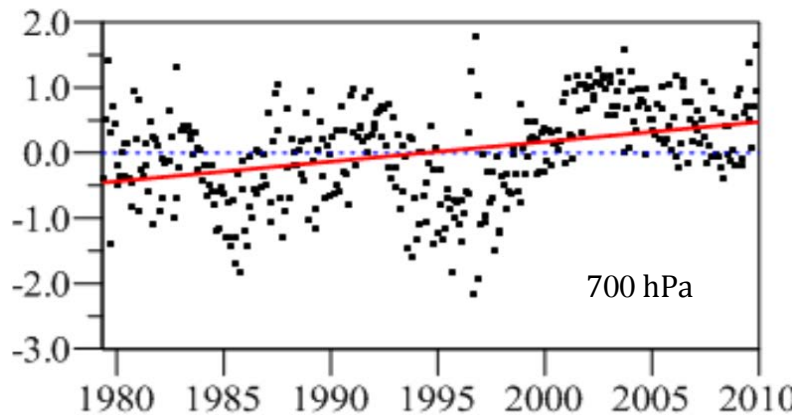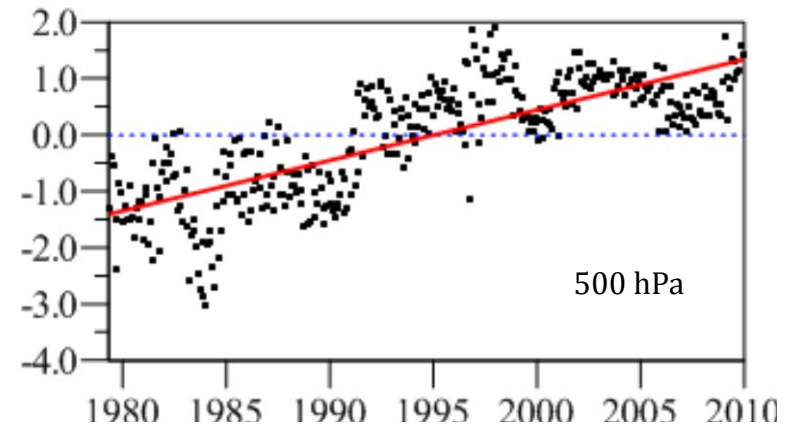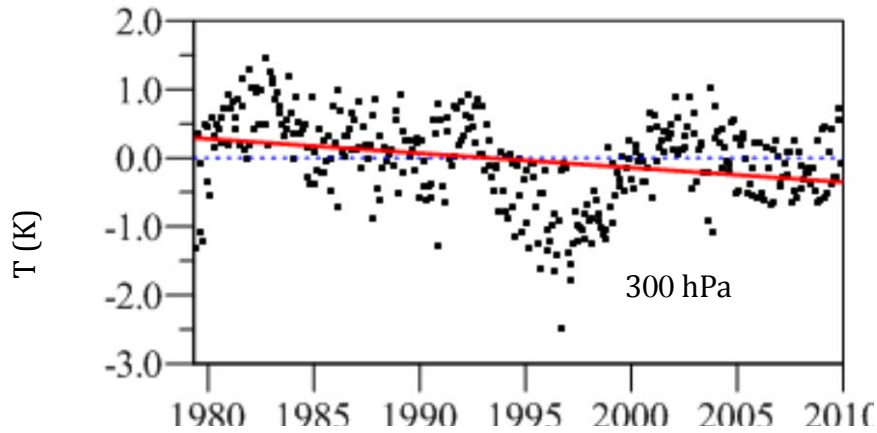
Mean Temperature Trends from 1990 to 2010 at Different Pressure Levels (3/3)
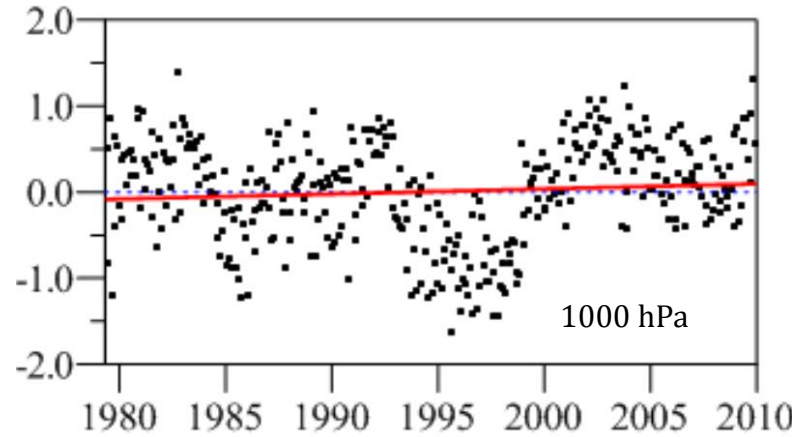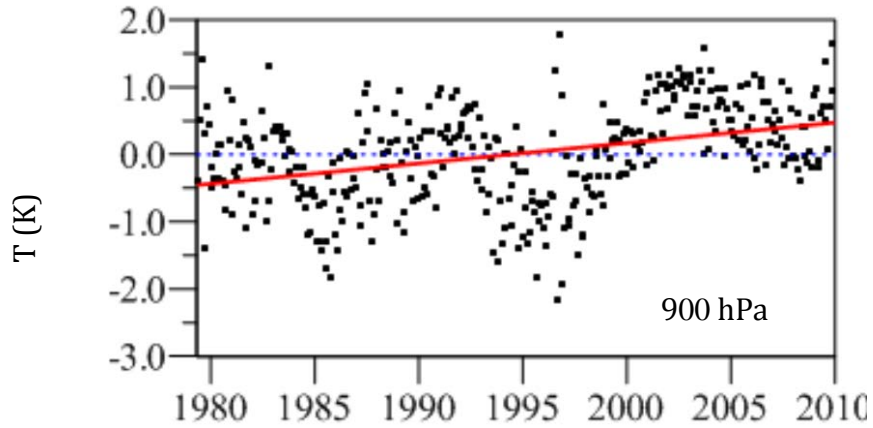
1D-Var Derived Temperature Trend

T Trend from 1D-Var
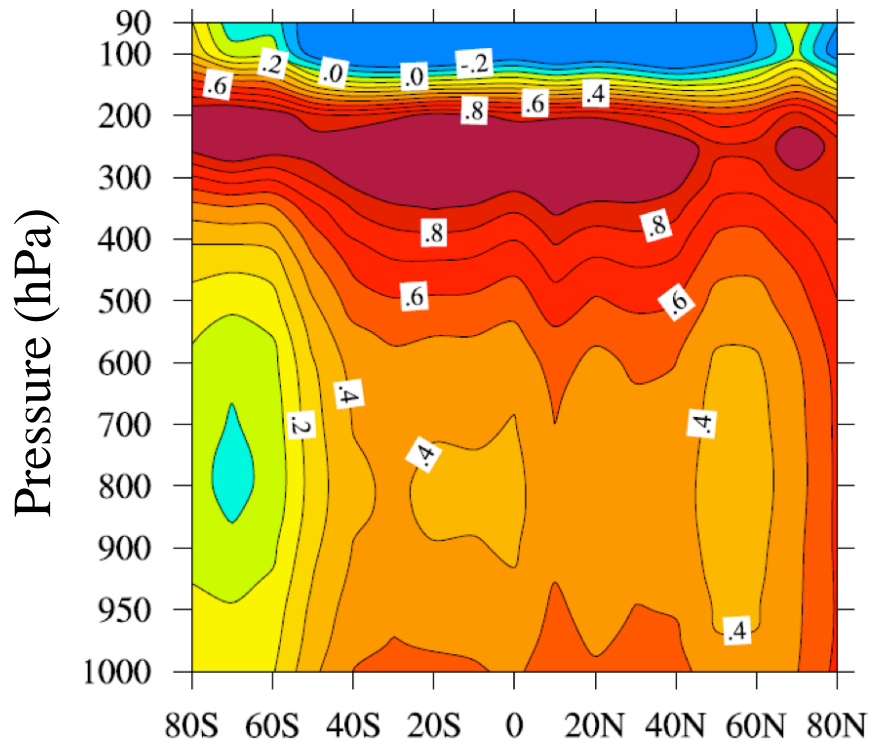
T$_b$ Trend from MSU/AMSU
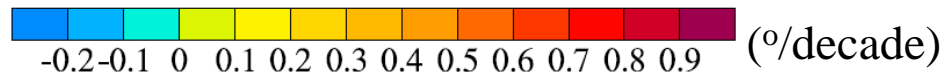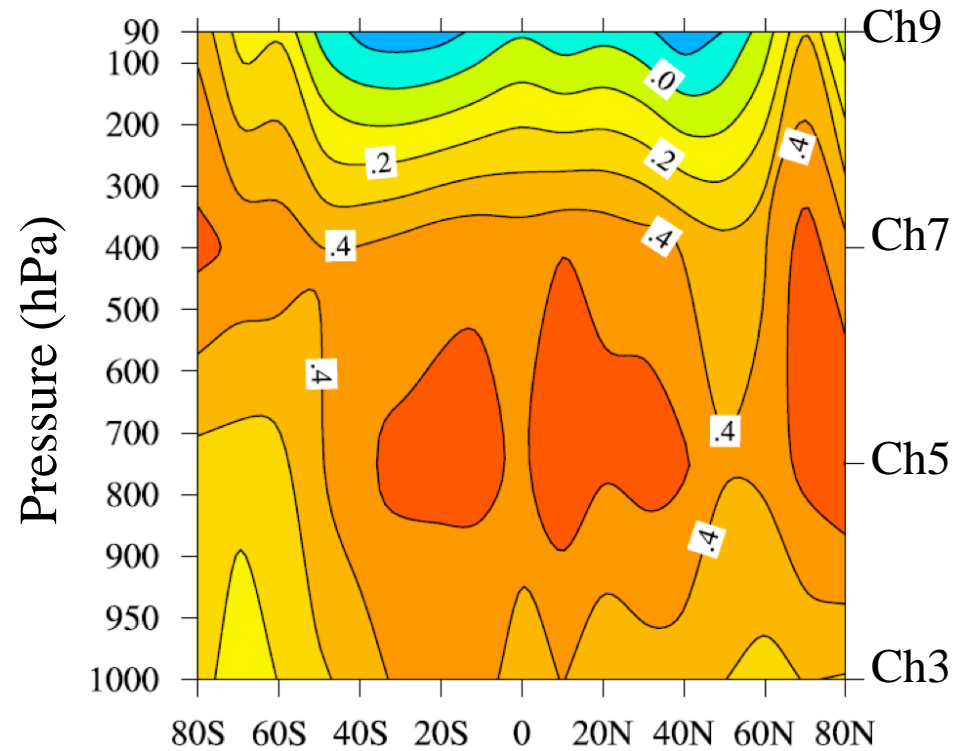
Weng, F. and X. Zou, 2013: 30-year atmospheric temperature trend derived by one-dimensional variational data assimilation of MSU/AMSU-A observations. *Clim. Dyn.*, DOI: 10.1007/s00382-013-2012-5.

Climate Model Derived Temperature Change from Doubling CO2

Meridional Winds [TCO2 — Control]
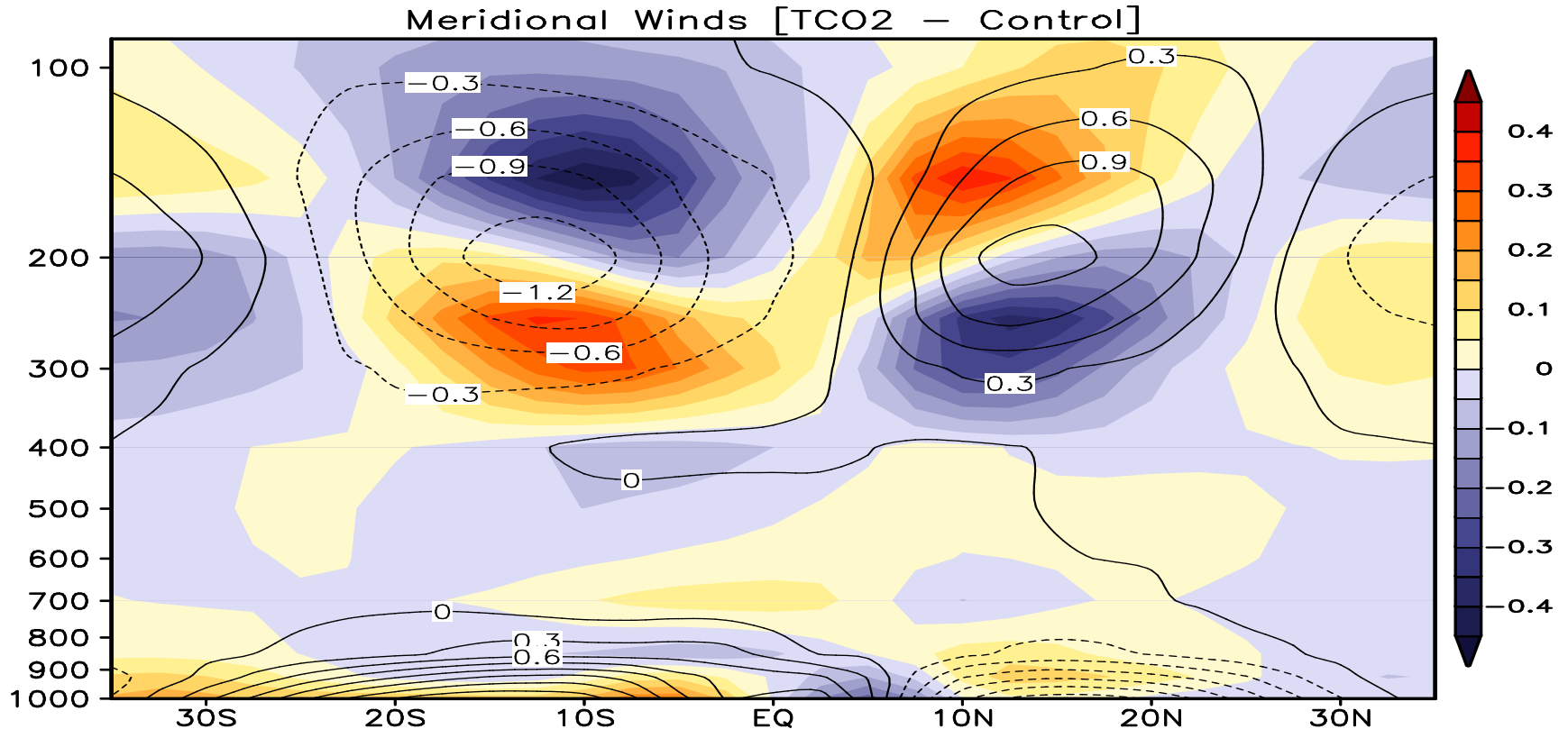
Lau and Kim, 2012: The Russian heat wave and Pakistan flood 2010: A teleconnection of hydroclimate extremes.. *J. Hydro. Meteor.*

Lau et al. 2013: A Canonical Response of Rainfall Characteristics to Global Warming, *Geophys. Res. Lett.*

Lau and Kim, 2014: A Robust Response of the Hadley Circulation to Global Warming, *Nature Geoscience (submitted)*

Summary and Conclusions

- Satellite measurements have become critical mass in global observing systems for both weather and climate applications

- For creating the climate data records from historical satellite instruments such as MSU, AMSU and ATMS, robust algorithms are required for calibration and data harmonization

- Atmospheric temperature trends derived satellite radiance data could be significantly different, compared to those in radiance space

- The scattering from precipitating clouds at 50-60 GHz primarily affects the AMSU derived tropospheric trends in both radiance and physical temperature spaces

- A significant atmospheric warming near tropopause is found from MSU-1dvar and is more consistent with the climate modeling results with doubling CO_2

More details can be found in

Zou, X., F. Weng and H. Yang, 2014: Connecting the time series of microwave sounding observations from AMSU to ATMS for long-term monitoring of climate change, *J. Ocean Atmos. Tech.*, (revised)

Yang, H. and X. Zou, 2014: Optimal ATMS remapping algorithm for climate research. *IEEE Trans. Geo. Remote Sensing,* in press

Weng, F., X. Zou and Z. Qin, 2013: Uncertainty of AMSU-A derived temperature trends in relationship with clouds and precipitation. *Clim. Dyn.*, DOI 10.1007/ s00382-013-1958-7.

Weng, F. and X. Zou, 2013: 30-year atmospheric temperature trend derived by one-dimensional variational data assimilation of MSU/AMSU-A observations. *Clim. Dyn.*, DOI: 10.1007/s00382-013-2012-5.

Qin, Z., X. Zou, and F. Weng, 2012: Comparison between linear and nonlinear trends in NOAA-15 AMSU-A brightness temperatures during 1998–2010, *Clim. Dyn.*, 10.1007/s00382-012-1296